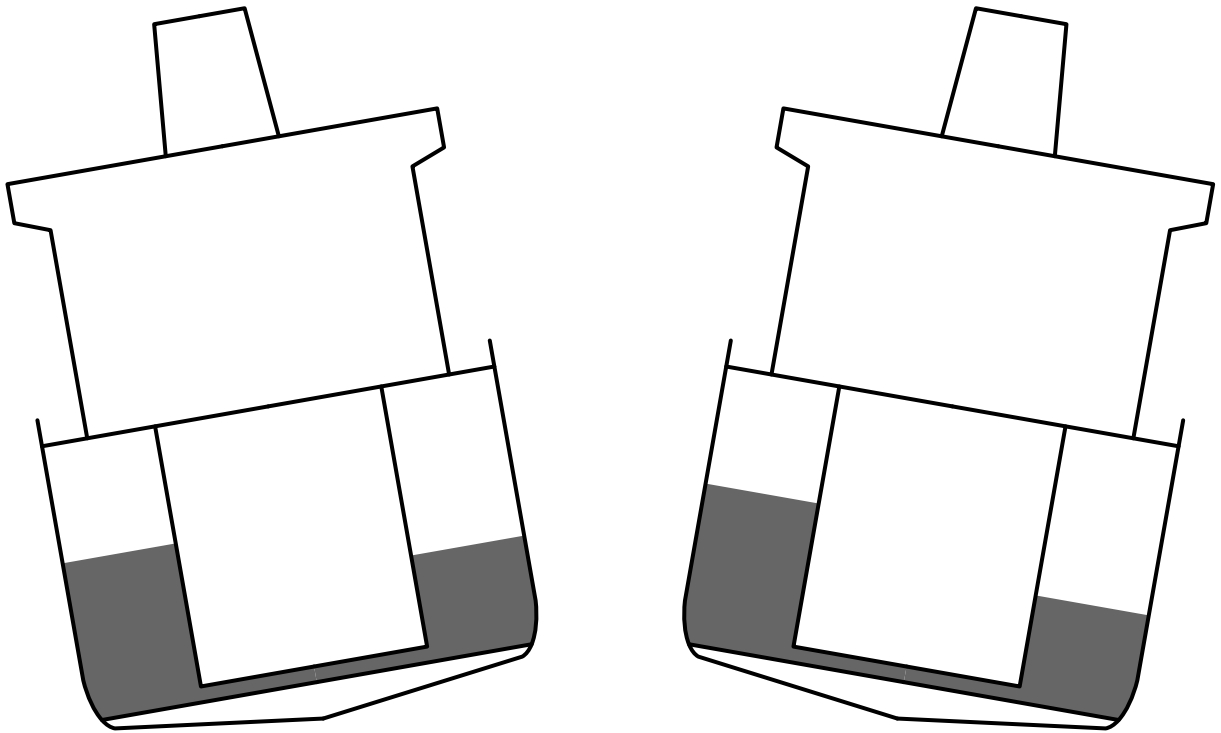


Numerical Simulation of Ship Motion Stabilization by an Activated U-tube Anti-Roll Tank

Theresa Kleefsman



Department of Mathematics
University of Groningen
P.O. Box 800
9700 AV Groningen

August 2000

Contents

1	Introduction	3
2	Mathematical Model	7
2.1	Navier-Stokes equations	7
2.2	Boundary conditions	8
2.2.1	The walls of the tank	8
2.2.2	The free surface	8
2.3	Forces and moments	9
3	Numerical Model	11
3.1	Apertures and VOF-function	11
3.2	Labeling	12
3.2.1	Geometry labels	12
3.2.2	Free-surface labels	13
3.3	Discretized Navier-Stokes equations	14
3.3.1	Time discretization	14
3.3.2	Spatial discretization	15
3.4	Solution method	16
3.4.1	Solution of the discrete Navier-Stokes equations	16
3.4.2	Volume of fluid convection and relabeling	17
3.4.3	Adaption of the time step using the CFL-number	18
4	Validation	19
4.1	Tests in irregular seas	19
4.1.1	Test circumstances	19
4.1.2	Input and output of ComFlo	20
4.1.3	Grid refinement study	20
4.1.4	Time step	20
4.1.5	Results	20
4.2	Decay tests	24
4.2.1	Experiment and test characteristics	24
4.2.2	Results	24
4.3	Tests in regular seas	30
4.3.1	Experiment characteristics	30
4.3.2	Input and output of ComFlo	30
4.3.3	Grid distribution and time step	31

4.3.4	Results	31
4.4	Conclusions about the validation	34
5	Controlled U-tanks	35
5.1	Physics of the control system	35
5.1.1	Passive operation	35
5.1.2	Controlled operation	36
5.2	Numerical model of the control system	36
5.2.1	Making the decision to close the valves	37
5.2.2	Determination of the closing time of the valves	37
5.2.3	Simulation of the closed valves	37
5.2.4	Opening the valves	38
5.3	Results	39
5.3.1	Valves closed for a fixed period of time	39
5.3.2	Stabilisation with the valves-based control system	41
6	Coupling with a linear two dimensional ship motion model	43
6.1	Linear 2DOF ship motion model	43
6.2	Numerical model of 2DOF ship motion model	45
6.3	Results	45
6.3.1	Excitation frequency near tank resonance	46
6.3.2	Various frequencies: no tank, passive tank and activated tank	47
7	Conclusions	49
A	Snapshots	51
B	Program Description	53
B.1	Calling sequence	53
B.2	Subroutines	53
B.3	Common block variables	55
B.4	Input files	59
B.5	Output files and post-processing	61
	Bibliography	65

Chapter 1

Introduction

A ship moving in the sea will rotate and displace under the influence of waves and wind. Already for a long time people are trying to stabilise ships. Especially they are trying to counteract the roll motion (which is the rotation about the longitudinal axis of the ship). Roll stabilisation is important for a number of reasons. First of all it provides more comfort for the crew and passengers, which is nice in every vessel. Besides this, roll stabilisation is desirable for pipe and cable-laying vessels. The operational conditions will improve when the roll motion can be stabilised. Furthermore a ship can sail faster when it suffers less from the roll motion.

There are several ways to decrease the roll motion, for example using fins or using tanks partially filled with water. A great disadvantage of using fins is that the effectiveness depends on the forward speed of the vessel. When the vessel has no speed, the fins do not give any stabilisation. Anti-roll tanks have a stabilising effect in both cases: for a vessel at rest or with forward speed. A few different tank designs are possible. Two types of anti-roll tanks are used in most cases: the open free surface tank and the U-tube tank. This report deals with the latter design.

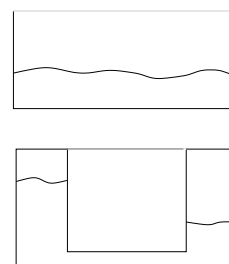


Figure 1.1: Top: open free surface tank; bottom: U-tube tank

A U-tube anti-roll tank (or U-tank) is a tank in U-shape, partially filled with water and thus has two smaller free surfaces in the wing tanks (see figure 1.2 for a picture of a U-tank in a ship). The design of the tank allows a U-tank to be installed in a vessel with little loss of space, which is an advantage of the design. The air exchange between both wing tanks is in most designs through a connecting air duct. A U-tank stabilises a ship by producing a counteracting moment. If the waves force the ship and tank to roll, the water in the tank is forced to flow. Because of the inertia of mass the motion of the water is delayed with respect to the roll motion of the vessel. So the moment produced by the tank water counteracts the excitation moment of the waves and the ship is forced to righten.

The largest counteracting moment occurs when the frequency of the roll motion is very much the same as the natural frequency of the U-tank. At other roll frequencies, the stabilising effect of the tank is much less and at some frequencies, the tank even causes an increase of

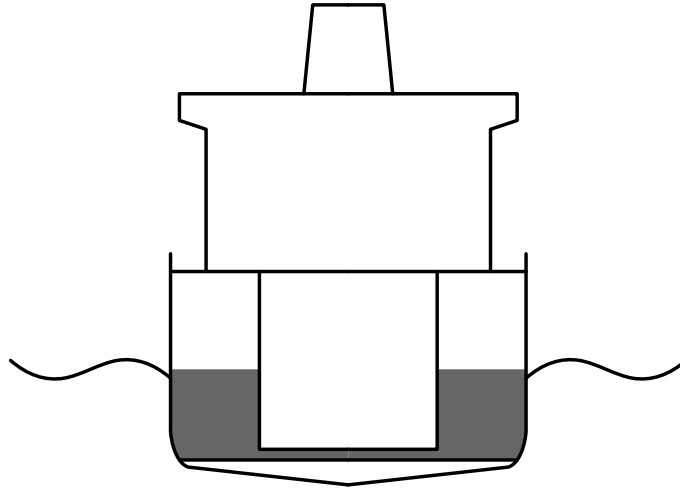


Figure 1.2: Cross section of a ship equipped with U-tank

the roll motion. This is why most of the U-tanks are extended with a control system which effectively changes the natural frequency of the tank. Examples of control systems are valves in the water duct or air duct that prevent the water from flowing, or pumps that force the water in the U-tank to flow in the desired direction. U-tanks without a control system are called passive, and tanks with a control system are called activated or controlled.

In the literature, detailed descriptions of anti-roll tanks can be found. An extensive research on U-tanks has been performed by Stigter [11], who gives equations of motion of the tank fluid and the tank-ship system. He compared his theory with experiments. An analysis of the influence of different parameters of anti-roll tanks can be found in the paper of Field and Martin [5]. They got their results by performing many experiments. Nowadays, with the increase of computer resources and improvement of numerical algorithms, experiments are more and more accompanied by computer simulations that are much cheaper to perform. Results of computer simulations of U-tanks can be found in papers of Zhong et al. [14] and Yamaguchi et al. [13]. In both papers not much attention is given to the validation of the computer programs they used.

In this master's thesis two dimensional simulations of the water flow in a U-tank are performed and studied. The simulations are carried out with the computer program ComFlo. ComFlo is able to simulate three dimensional fluid flow with free surfaces. It is based on the finite volume method. ComFlo is already validated extensively for the use of simulation of water flow in a free surface tank. The results of this validation program are presented in two reports: one for two dimensional simulation [3] and one for three dimensional simulation [4]. The goal of this master's thesis is to validate ComFlo for the use of two dimensional simulation of water flow in a passive and activated U-tank. Therefore ComFlo is first validated using experiments with passive U-tanks. Then a model of a control system is added to ComFlo. Finally, ComFlo is extended with a ship motion model to account for the coupling between the tank fluid motion and the ship motion.

This report consists of seven chapters and a program description in an appendix.

First, it gives the mathematical and numerical model used in the simulations in chapter 2 and 3. Then the results of the validation of ComFlo with respect to its use in simulation of fluid flow in a U-tank are presented in the fourth chapter. Chapter 5 deals with the control system: an explanation, the implementation and results. In chapter 6 the coupling of the ComFlo fluid simulations and a linear ship motion model is discussed. Finally, conclusions are drawn in chapter 7.

Chapter 2

Mathematical Model

2.1 Navier-Stokes equations

The motion of a fluid through a domain can be described by the Navier-Stokes equations. In our case the fluid is water. Water can be considered as an incompressible and viscous fluid. For the water motion, the Navier-Stokes equations describing the conservation of mass and momentum can be simplified to

- *conservation of mass*

$$\nabla \cdot \mathbf{u} = 0 \quad (2.1)$$

with $\mathbf{u} = (u, v, w)$ the velocity vector.

- *conservation of momentum*

$$\frac{\partial \mathbf{u}}{\partial t} + \nabla \cdot (\mathbf{u}\mathbf{u}^T) = -\frac{1}{\rho}\nabla p + \nu(\nabla \cdot \nabla)\mathbf{u} + \mathbf{F} + \mathbf{f} \quad (2.2)$$

In this equation, ν is the kinematic viscosity, ρ denotes density, which will be normalized to unity ($\rho = 1$). The pressure is denoted by p and \mathbf{F} stands for external forces (gravity for example). The symbol \mathbf{f} is a virtual body force which originates from the motion of the domain.

We take the Cartesian co-ordinate frame to be fixed to the ship and tank. But because the ship is moving due to the wave-forces, the ship-fixed frame is moving in an earth-fixed frame (see figure 2.1). Therefore a virtual body force \mathbf{f} is introduced in equation 2.2. This force is given by

$$\mathbf{f} = -\frac{d\mathbf{q}}{dt} - \boldsymbol{\omega} \times (\boldsymbol{\omega} \times \mathbf{r}) - \frac{d\boldsymbol{\omega}}{dt} \times \mathbf{r} - 2\boldsymbol{\omega} \times \mathbf{u},$$

with

- \mathbf{q} the velocity of the origin \mathcal{O} of the ship-fixed frame,
- $\boldsymbol{\omega}$ the angular velocity of the ship with respect to the earth-fixed frame,
- \mathbf{r} the translation vector from the ship-fixed frame.

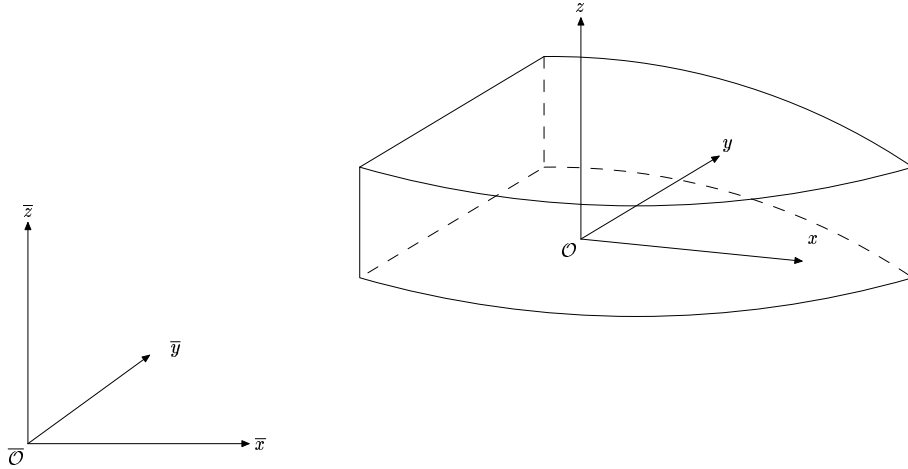


Figure 2.1: *Earth-fixed frame and ship-fixed frame*

2.2 Boundary conditions

Inside the tank, we have to solve the Navier-Stokes equations. But for solving differential equations, we need boundary conditions. Because the tank is only partially filled with water, we need boundary conditions at the walls of the tank and at the free surface.

2.2.1 The walls of the tank

At the walls of the tank we take a free slip boundary condition and demand that no fluid can go through the wall. In formula the boundary conditions at the wall are given by

$$\frac{\partial u_t}{\partial \mathbf{n}} = 0 \quad (2.3)$$

$$u_n = 0. \quad (2.4)$$

where $u_t = \mathbf{u} \cdot \mathbf{t}$ denotes the velocity tangential to the wall and $u_n = \mathbf{u} \cdot \mathbf{n}$ is the velocity normal to the wall (\mathbf{n} is the normal direction). They describe the free slip condition and the condition that no fluid can go through the wall respectively.

2.2.2 The free surface

At a free surface, we guarantee continuity of tangential and normal stresses by prescribing boundary conditions. If we assume the fluid is incompressible and we neglect the capillary effects, these boundary conditions are given by ([12])

$$-p + 2\mu \frac{\partial u_n}{\partial \mathbf{n}} = -p_0 \quad (2.5)$$

$$\mu \left(\frac{\partial u_n}{\partial \mathbf{t}} + \frac{\partial u_t}{\partial \mathbf{n}} \right) = 0 \quad (2.6)$$

where μ denotes the dynamical viscosity and p_0 the atmospheric pressure.

By neglecting viscous effects, equation 2.6 is simplified to

$$p = p_0 \tag{2.7}$$

at the free surface. This makes the numerical model much easier. Equation 2.6 is modified as well. In two dimensions, in this case in the y, z -plane, $\frac{\partial w}{\partial y} + \frac{\partial v}{\partial z} = 0$ is prescribed. This is exact if we have only horizontal and vertical walls. In three dimensions we use a similar simplification. Then equation 2.6 is modified to

$$\frac{\partial w}{\partial y} + \frac{\partial v}{\partial z} = 0 \text{ or } \frac{\partial u}{\partial z} + \frac{\partial w}{\partial x} = 0 \text{ or } \frac{\partial v}{\partial x} + \frac{\partial u}{\partial y} = 0.$$

where the one 'closest' to 2.6 is used in the actual situation. The advantage of this simplification is that these conditions are much easier to compute on a Cartesian grid.

2.3 Forces and moments

The fluid in a flow domain induces a force on an object in the domain. This force normally consists of two parts, namely the pressure force and the shear force. In this report, the shear force is neglected, because it is much smaller than the pressure force. The pressure force is calculated as the integral of the pressure along the boundary of the object S . This results in the formula:

$$\mathbf{F}_p = \int_S p \mathbf{n} dS.$$

The forces induce a moment, which can be calculated if the force on the object is split up into the three co-ordinate directions. Then the moment with respect to the center of mass of the solid tank will be calculated as follows:

$$\mathbf{M} = \mathbf{r} \times \mathbf{F}$$

with \mathbf{r} the distance from the point on which the force is exerted to the center of mass.

Chapter 3

Numerical Model

To perform computer simulations of fluid flow, the flow domain is covered by a Cartesian grid. In every cell of the grid that contains fluid, the discretized Navier-Stokes equations will be solved. Therefore we must know which cell contains fluid, which is a boundary or free surface cell and which is an exterior cell. To indicate this the cells will be labeled. After this, the Navier-Stokes equations must be discretized and solved. In this chapter we will give the details of the numerical model. This chapter is almost literally taken from the master's thesis of Jeroen Gerrits [7]. We will explain most of the numerical method in two dimensions.

3.1 Apertures and VOF-function

As mentioned above we cover the (arbitrary) flow domain Ω , in two- or three-dimensional space, with a Cartesian grid. The computational cells of the grid are cut by the curved boundary of Ω in a wide variety. Hence cells with different characters originate. This difference in character is incorporated in the numerical method by introducing *apertures* [10].

In the centre of every computational cell a *volume-aperture* F^b is defined which indicates the fraction of the cell-volume that is open to flow (so $0 \leq F^b \leq 1$). Analogously we define in the centre of every cell-face an *edge-aperture* A^x (in x -direction) or A^y (in y -direction). Of course in 3-D a third edge-aperture A^z is introduced. We note that edge-apertures contain information that is one dimension lower than the information given by volume-apertures (e.g. three-dimensional edge-apertures indicate the fraction of a *cell-surface* open to flow, which is two-dimensional information). The use of apertures is illustrated in figure 3.1. The apertures F^b , A^x and A^y (and A^z in 3-D) are used to discretize the Navier-Stokes equations near the boundary and to compute the boundary velocities (see sections 3.4 and 3.6 in [6]).

Since Ω is partially filled with fluid we need additional information to be able to trace the free surface. This is accomplished by introducing one more volume-aperture F^s (also defined in the centre of every cell) better known as a volume of fluid (VOF) function [9]. This (discrete) function indicates the fraction of a computational cell that is occupied by fluid. As a consequence we have $F^s \leq F^b$ throughout the computational grid. An important difference between the volume-aperture F^b and the VOF function F^s is the time-dependency. As F^b can be computed once before the start of the time integration, the VOF function has to be adjusted every single time step. This procedure is explained in section 3.4.2.

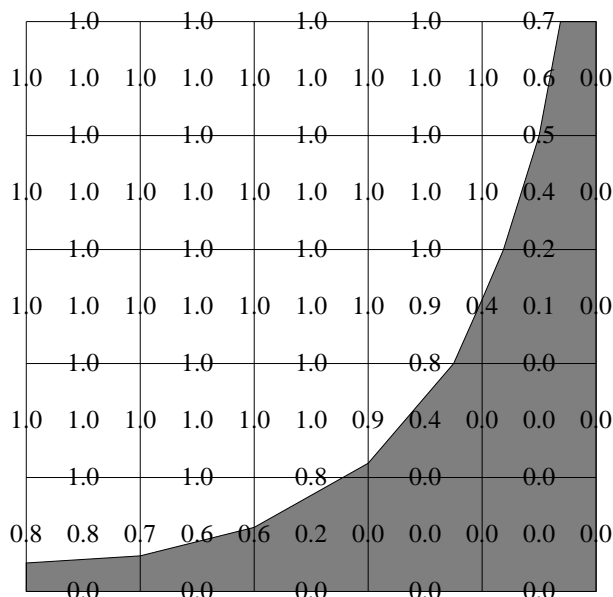


Figure 3.1: *Example of a (discrete) aperture-field (rounded to one decimal place).*

3.2 Labeling

The continuity equation 2.1 and momentum equations 2.2 are discretized on a staggered grid, i.e. the continuity equation is discretized in cell-centres while the velocity components are solved from the momentum equations in the centre of cell-faces.

In section 3.2 of [6] two different methods are examined to apply the boundary conditions. In the first (conventional) method all the boundary velocities (i.e. velocities solved from the solid boundary conditions) were located outside the flow domain, while the second method used some boundary velocities inside the flow domain. The latter turned out to have some advantages compared to the former. For example the second method does not cause stability problems in contrast to the first method. This is the reason why in this report the second method is chosen to set up the numerical model (this method is explained in the section below). Further some new labels are introduced as compared to [6], since the current model includes free-surface flow (section 3.2.2).

3.2.1 Geometry labels

Prior to the time integration the cells are labeled on the basis of the geometry only. First all cells with $F^b \geq \frac{1}{2}$ are labeled as an **F**(low)-cell. This means that at least half of an **F**-cell is open to flow. A computational cell adjacent to an **F**-cell but with $F^b < \frac{1}{2}$ will be called a **B**(oundary)-cell. Finally all the remaining cells are labeled as an **X**()-cell (from exterior). These cells have no significant role in the numerical model.

Based on the cell labeling the velocities are labeled by a combination of two letters; for example a velocity component between an **F**- and a **B**-cell will be called an **FB**-velocity. The geometry labels are illustrated in figure 3.2.

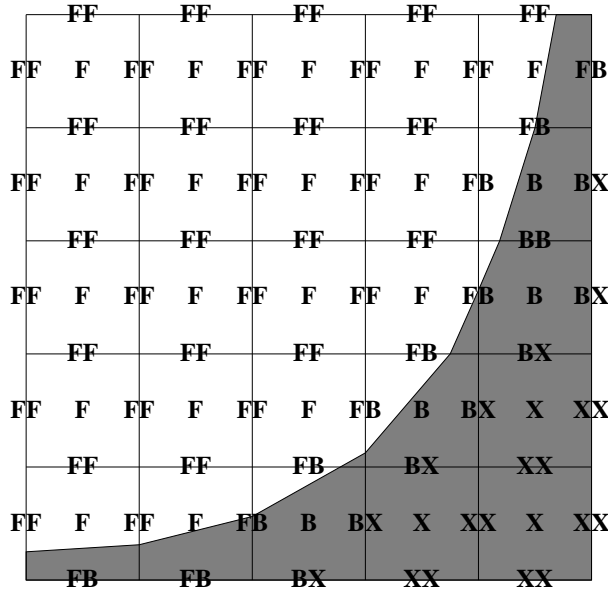


Figure 3.2: Cell and velocity labels based on geometry only.

3.2.2 Free-surface labels

The geometry labels are the basis of a more comprehensive labeling to be able to trace the free surface. Since the **B**- and **X**-cells consist of more than 50% solid boundary these labels remain unchanged during the rest of the computational process. Thus, every time step, only the **F**-cells have to be examined on the occurrence of liquid. If a cell contains no fluid, i.e. $F^s = 0$, then the cell is called an **E**(mpty)-cell. All the cells adjacent to an **E**-cell with $F^s > 0$ are labeled as an **S**(urface)-cell.¹ The remaining **F**(low)-cells now will be called **F**(luid)-cells. Figure 3.3 illustrates the free-surface labels in combination with the geometry labels.

Based on the cell labels we decide the following:

- In **E**-, **B**- and **X**-cells no pressure is computed or prescribed since these cells contain (almost) no fluid.
- At the free surface, the pressure is equal to the atmospheric pressure according to the free surface condition 2.7. Then the pressure in **S**-cells is calculated by inter- or extrapolating the atmospheric pressure at the free surface and the pressure in an adjacent **F**-cell.
- In all the **F**-cells the pressure is solved from the continuity equation 2.1 or to be more precise from the pressure Poisson equation (see section 3.4).

The velocities are labeled by a combination of two letters as in the previous section. A priori 15 different combinations can be made. However an **X**-cell can not be adjacent to an **F**-, **S**- or **E**-cell and an **F**-cell can not be next to an **E**-cell. Further **BX**- and **XX**-velocities are ignored since these are not needed in the finite-difference formulas representing the first- and second-order derivatives in the Navier-Stokes equations. Thus only the following 9 combinations remain for further study:

¹In the computer program a cell is labeled an **E**-cell if $F^s < \varepsilon$, with ε a small constant, to take rounding errors into account. Analogously an **S**-cell satisfies $F^s \geq \varepsilon$.

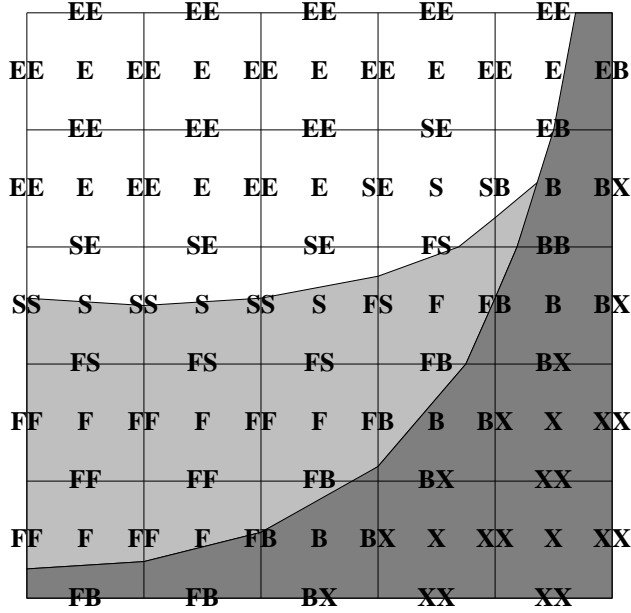


Figure 3.3: *Free-surface labels and geometry labels.*

- **FF**, **FS**, **SS**, **SE** and **EE**. Based on only the geometry these are the **FF**-velocities.
- **FB**, **SB** and **EB**. These are the **FB**-velocities if only the geometry labels are considered.
- **BB**.

Since in both the **F**-cells and the **S**-cells a pressure is defined a pressure gradient can be computed between two **F**-cells, between an **F**- and an **S**-cell and between two **S**-cells. Hence all the **FF**-, **FS**- and **SS**-velocities are solved from the momentum equations. In the remainder of this report we will call these velocities *momentum velocities*. We will call the **SE**- and **EE**-velocities *free-surface velocities* and the rest of the velocities (**FB**, **SB**, **EB** and **BB**) are the *boundary velocities*. An explanation of how these velocities are calculated and used is given in [6] and [7].

3.3 Discretized Navier-Stokes equations

In this section we will discuss the discretization of 2.1 and 2.2.

3.3.1 Time discretization

In [6] it has been shown that the labeling method as discussed in the previous section does not cause stability problems. Hence the Navier-Stokes equations are discretized explicit in time. If we use the most elementary time integration method *forward Euler* we get:

$$\operatorname{div} \mathbf{u}^{n+1} = 0, \quad (3.1)$$

$$\frac{\mathbf{u}^{n+1} - \mathbf{u}^n}{\delta t} + \operatorname{grad} p^{n+1} = \nu \operatorname{div} \operatorname{grad} \mathbf{u}^n - \operatorname{div} (\mathbf{u}^n \mathbf{u}^{nT}) + \mathbf{F}^n + \mathbf{f}^n, \quad (3.2)$$

where δt is the time step, \mathbf{u}^n the velocity field at time $t_n = n \cdot \delta t$ and p^{n+1} the pressure distribution at time t_{n+1} . The pressure gradient is discretized at the ‘new’ time level to ensure that the ‘new’ velocity field from 3.2 is divergence-free.

3.3.2 Spatial discretization

The time-discretized equations 3.1 and 3.2 have to be discretized in space as well. This procedure is exactly the same as in [6]. Hence we only give here the main features of the spatial discretization.

For the spatial discretization conservation cells are used. In these cells both conservation of mass and momentum is required. The conservation cell for the continuity equation is identical to a computational cell, while a conservation cell for the momentum equations consists of two computational cells (see figures 3.4 and 3.5 respectively). Since the continuity equation

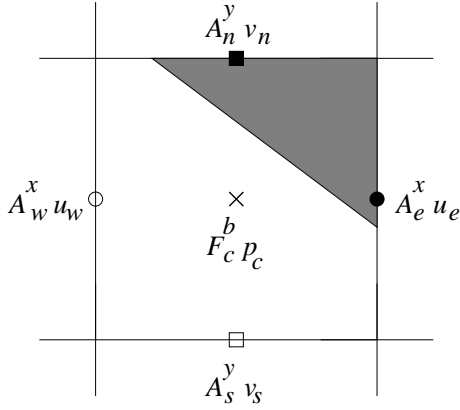


Figure 3.4: Conservation cell for the continuity equation.

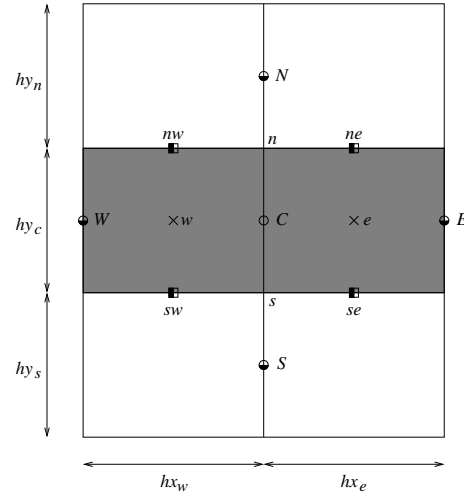


Figure 3.5: Conservation cell for the momentum equation in x -direction.

expresses that the net amount of mass flowing through the boundary of a computational cell must be equal to zero the continuity equation is discretized based on apertures. This way we take into account that no mass can flow through the solid boundary.

The same applies to the convective terms of the momentum equations. These indicate the increase of momentum in a conservation cell because of transport of momentum through the boundary of that cell. Since momentum cannot flow through $\partial\Omega$ the convective terms are discretized based on apertures too. The diffusive terms, the pressure gradient and the body forces indicate the increase of momentum due to stresses rather than transport. Hence these terms in the momentum equations are *not* discretized with apertures.

The above-mentioned results in the following discretized Navier-Stokes equations:

$$D_h^a \mathbf{u}^{n+1} = 0, \quad (3.3)$$

$$\frac{\mathbf{u}^{n+1} - \mathbf{u}^n}{\delta t} + G_h p^{n+1} = \nu D_h G_h \mathbf{u}^n - D_h^a (\mathbf{u}^n \mathbf{u}^{nT}) + \mathbf{F}^n + \mathbf{f}^n. \quad (3.4)$$

Here D_h and G_h are the discrete versions of the divergence and gradient operators. D_h^a indicates that the divergence operator is discretized with apertures. The solution of equations 3.3 and 3.4 is discussed in section 3.4.

3.4 Solution method

In this section we will show how the discrete Navier-Stokes equations are solved, which algorithm is used to ‘move’ the fluid and how the time step will be adapted. First some notation is introduced. The set of points in the computational grid where a momentum velocity (**FF**, **FS** and **SS**) is defined will be denoted by Ω_h^f (roughly spoken the points inside the fluid). Further Ω_h^s contains the free-surface velocities (**SE** and **EE**) and Ω_h^b contains the boundary velocities (**FB**, **SB**, **EB** and **BB**). Finally we define $\Omega_h = \Omega_h^f \cup \Omega_h^s \cup \Omega_h^b$ as the entire computational grid (see figure 3.6). We note that the sets Ω_h^f and Ω_h^s vary in time whereas Ω_h^b is time-independent.

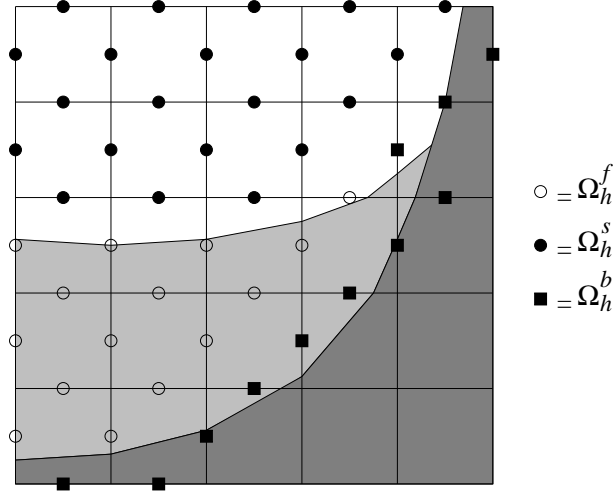


Figure 3.6: *Momentum, free-surface and boundary velocities.*

3.4.1 Solution of the discrete Navier-Stokes equations

We assume an initial velocity field \mathbf{u}^n is given on Ω_h (for $n = 0$ we simply take $\mathbf{u}^0 = 0$). Our goal is to compute a new velocity field \mathbf{u}^{n+1} and a new pressure distribution p^{n+1} from the discrete Navier-Stokes equations 3.3 and 3.4.

First in all the **S**-cells the pressure is set equal to the atmospheric pressure

$$p = p_0 \text{ in } \mathbf{S}\text{-cells,}$$

and a temporary vector field $\tilde{\mathbf{u}}$ is created on Ω_h^f by integrating the momentum equations 3.4 without the pressure gradient, i.e.

$$\tilde{\mathbf{u}} = \mathbf{u}^n + \delta t \left\{ \nu D_h G_h \mathbf{u}^n - D_h^a \left(\mathbf{u}^n \mathbf{u}^{nT} \right) + \mathbf{F}^n + \mathbf{f}^n \right\} \text{ on } \Omega_h^f. \quad (3.5)$$

Note that $\tilde{\mathbf{u}}$ is *not* a velocity field. At this stage \mathbf{u}^{n+1} on Ω_h^f and p^{n+1} in all the **F**-cells have to be solved from

$$D_h^a \mathbf{u}^{n+1} = 0 \text{ in } \mathbf{F}\text{-cells}, \quad (3.6)$$

$$\mathbf{u}^{n+1} + \delta t G_h p^{n+1} = \tilde{\mathbf{u}} \text{ on } \Omega_h^f. \quad (3.7)$$

The operator D_h^a works on unknown velocities in Ω_h^f and Ω_h^b , i.e. on momentum and boundary velocities. Hence 3.7 cannot be substituted directly into 3.6 since then the pressure in **B**-cells would be needed; remember that the continuity equation is discretized in **F**-cells while **FB**-velocities are not solved from the momentum equations [12]. This problem does not occur at the free surface because **FS**-velocities are solved from the momentum equations. To avoid this problem of the missing boundary condition for the pressure we write

$$D_h^a = D_h^{a,f} + D_h^{a,b},$$

where $D_h^{a,f}$ and $D_h^{a,b}$ operate on velocities in Ω_h^f and Ω_h^b respectively. Yet the problem is not solved because we can not compute the boundary velocities at the new time level since therefore we would need the entire velocity field at the new time level. That is why these velocities are set equal to the boundary velocities at the old time level, i.e. $\mathbf{u}^{n+1} = \mathbf{u}^n$ on Ω_h^b . This procedure causes an error $\mathcal{O}(\delta t)$ which already has been introduced by the time integration method forward Euler. Then it remains to solve

$$D_h^{a,f} \mathbf{u}^{n+1} = -D_h^{a,b} \mathbf{u}^n \text{ in } \mathbf{F}\text{-cells}, \quad (3.8)$$

$$\mathbf{u}^{n+1} + \delta t G_h p^{n+1} = \tilde{\mathbf{u}} \text{ on } \Omega_h^f. \quad (3.9)$$

Now it is possible to substitute 3.9 into 3.8 resulting in the *pressure Poisson equation*

$$D_h^{a,f} G_h p^{n+1} = \frac{1}{\delta t} \left(D_h^{a,b} \mathbf{u}^n + D_h^{a,f} \tilde{\mathbf{u}} \right) \text{ in } \mathbf{F}\text{-cells}, \quad (3.10)$$

which has to be solved in every **F**-cell in order to produce a new pressure distribution p^{n+1} . The pressure Poisson equation is solved by SOR-iteration (Successive Over-Relaxation) with automated adjustment of the relaxation parameter. The solution of 3.10 is then used to compute the new momentum velocities

$$\mathbf{u}^{n+1} = \tilde{\mathbf{u}} - \delta t G_h p^{n+1} \text{ on } \Omega_h^f. \quad (3.11)$$

Finally the free-surface velocities and boundary velocities are adjusted such that the new velocity field \mathbf{u}^{n+1} has been computed on the entire grid Ω_h .

3.4.2 Volume of fluid convection and relabeling

Once a new velocity field has been computed the position of the fluid has to be changed based on this velocity field. Hereto the donor-acceptor method [9] has been implemented and slightly adjusted to account for the complex geometries.

In the current labeling method fluid can flow from an **F**- or **S**-cell towards an **F**-, **S**- or **E**-cell. Hence at every cell-face with label **FF**, **FS**, **SS** or **SE** a flux is computed indicating the amount of fluid flowing from the donor to the acceptor cell during one time step.

After the volume of fluid convection the cells and velocities are relabeled based on the new volume of fluid distribution. At this stage at the end of the time cycle, the time step will be adapted using the CFL-condition as explained below.

3.4.3 Adaption of the time step using the CFL-number

For stability, the time step must satisfy a condition:

$$\frac{|u| \delta t}{h} \leq 1$$

with u the velocity, δt the time step and h the cell width. The left hand side of the equation is called the CFL-number.

Every time step ComFlo computes the CFL-number in the following way:

$$\text{CFL} = \max \left(\frac{|u| \delta t}{h_x}, \frac{|v| \delta t}{h_y}, \frac{|w| \delta t}{h_z} \right).$$

This CFL-number is computed to see if it is less than a **CFLmax** which is given by the user. If it is greater than **CFLmax**, the time step will be halved. If ten time steps in a row the CFL number is below a given **CFLmin** the time step is doubled.

At this stage one time cycle has been completed and the entire process is repeated until the maximum simulation time has been reached.

Chapter 4

Validation

In this chapter the validation of ComFlo is presented. The results of three types of experiments were available for the validation. The first type consists of experiments carried out by Marin in irregular seas. The second type is decay tests, which shows us how ComFlo predicts the internal damping of the U-tank. The last type is experiments in regular seas, that come from a paper by Field and Martin [5].

4.1 Tests in irregular seas

4.1.1 Test circumstances

The tests have been carried out in irregular seas by Marin for a Fishing Patrol Vessel. The dimensions of the U-tank which was used are given in figure 4.1. At time $t = 0$ the water in the tank is at rest.

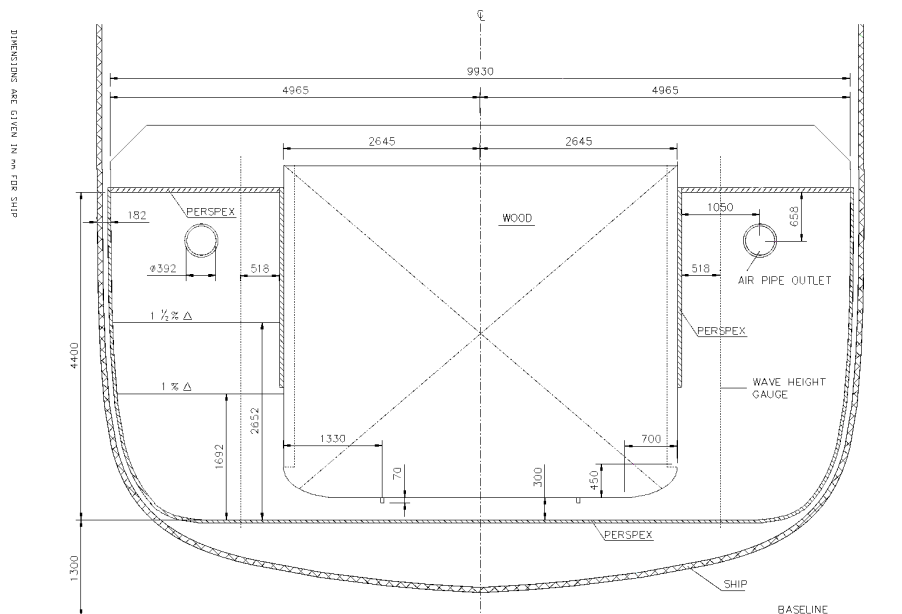


Figure 4.1: *Ship and U-tank, cross-sectional view*

We will give the results of one typical test. The conditions of this experiment are given in the table below.

speed of vessel [knots]	Duct height [m]	Water volume [m^3]	water height PS column at $t = 0$ [m]	water height SB column at $t = 0$ [m]
0.0	0.3	15.1	-0.533	0.527

4.1.2 Input and output of ComFlo

In the experiments, the motion of the ship and the motion of the water in the tank are measured. The motion of the ship is input for ComFlo. Then ComFlo computes the motion of the water in the tank. The ship motion is given in the input files `sway_ms.dat`, `heave_ms.dat` and `roll_ms.dat` that contain the motion, velocity and acceleration of the sway, heave and roll movement of the ship respectively. As output, ComFlo produces data, among them the water height in the wing tanks, the sway and heave force and the roll moment, which can be compared with the experimental data.

4.1.3 Grid refinement study

To determine a suitable number of grid points in each direction, we performed a grid refinement study. For that purpose we simulated an experiment in irregular seas on three different grids: a grid of 50x22 points, of 100x44 points and of 200x88 points. In figure 4.2 the roll moment of the test described above calculated on three different grids can be found. The results of the coarse grid of 50x22 points are not satisfactory. The results of the finer grids of 100x44 and 200x88 points are pretty much the same. So, a grid of 100x44 grid points has been chosen to perform the simulations. In figure 4.3 the geometry and grid distribution are shown.

4.1.4 Time step

The simulations have been started with an initial time step of 0.01 second. ComFlo adapts the time step every time using the CFL-number (see section 3.4.3). Figure 4.4 presents the evolution of the time step during the first 100 seconds of the simulation. In the first few seconds the time step gets very large. This is because we start with an initial velocity field of 0 m/s.

4.1.5 Results

Five full simulations of different experiments have been done. In Appendix A snapshots of the velocity field of a part of a simulation in irregular seas are given. We will give the results of the first 500 seconds of only one of the simulations, because the simulations are pretty much the same. The results of the simulation are presented in time histories of the water height in the port side tank, sway force, and roll moment with respect to the ship's center of mass. The calculated results are compared with the experimental test results. The agreement between the computer simulations and the experiments is very good. Almost no phase difference occurs and the amplitudes are predicted well too.

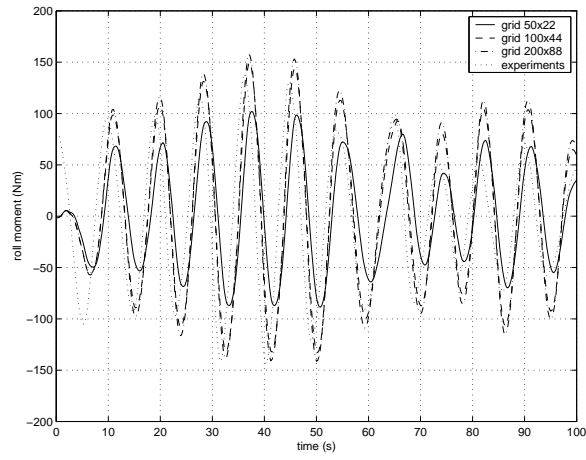


Figure 4.2: *Grid refinement study*



Figure 4.3: *Geometry and 100x44 grid used with the simulations*

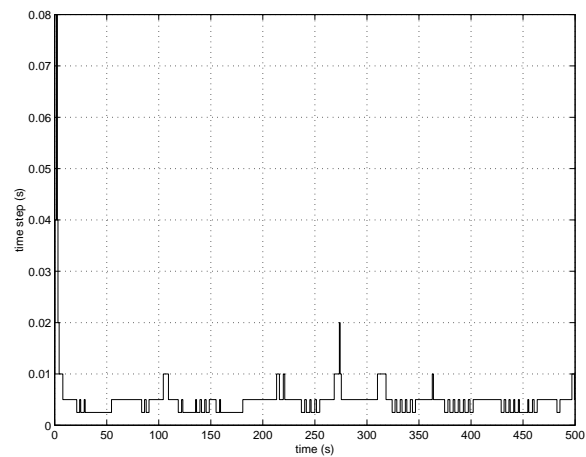


Figure 4.4: *Evolution of the time step during the simulation in irregular seas*

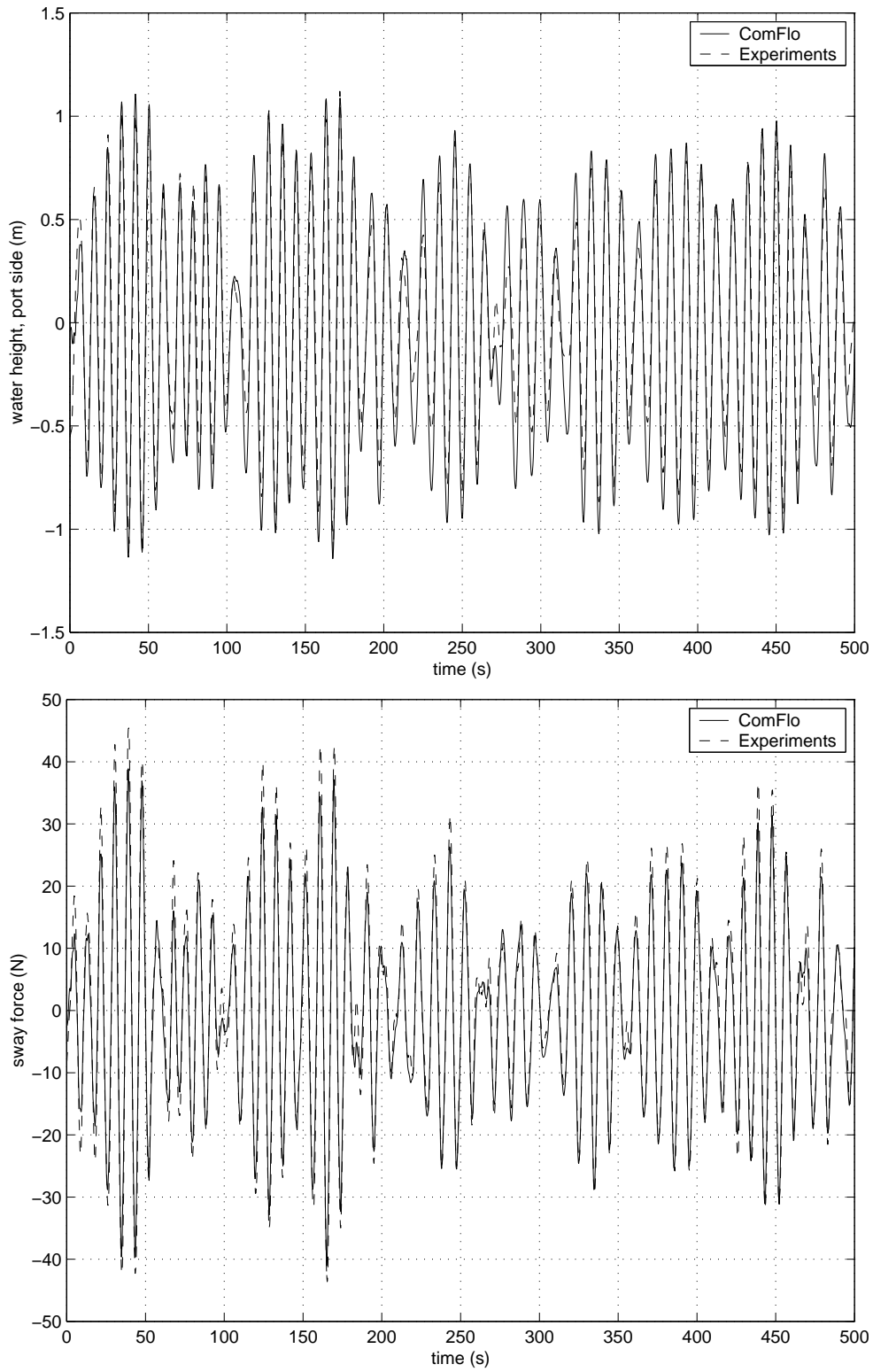


Figure 4.5: *U-tank*, top: water height in PS tank; bottom:sway force

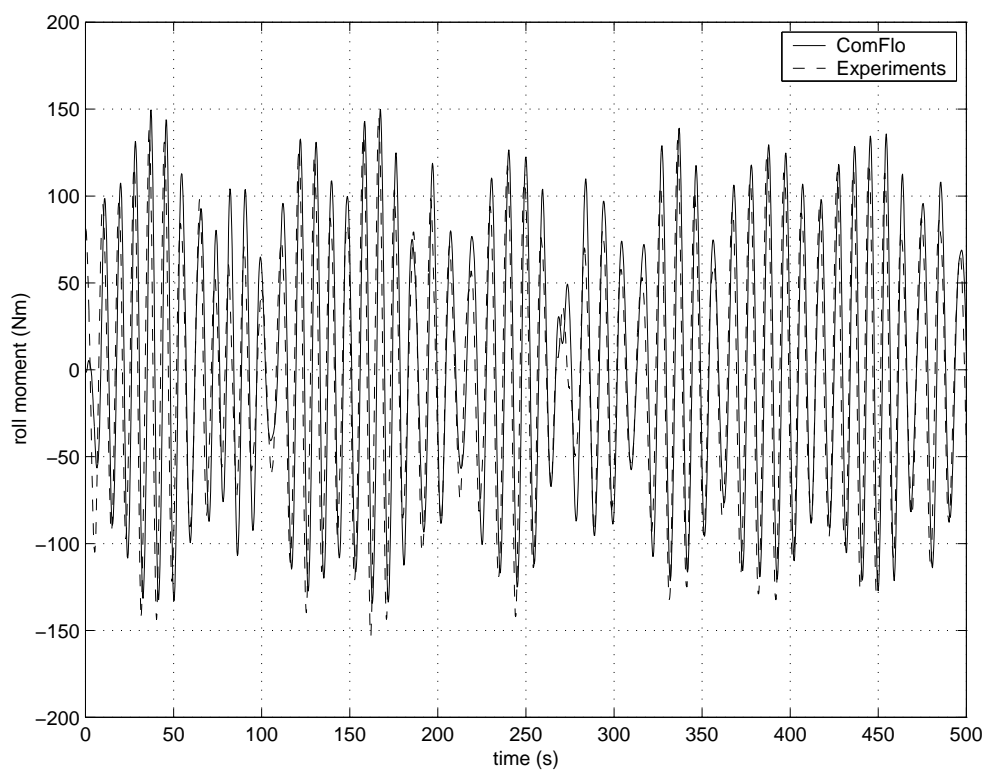


Figure 4.6: *U-tank, roll moment*

4.2 Decay tests

4.2.1 Experiment and test characteristics

The decay tests have been carried out with the same tank as in the tests above. The ship (with tank) is given a roll amplitude and released. Then the U-tank starts to decay.

We performed simulations of seven decay tests. In the table below the conditions of the two tests from which we will show the results in this report are given.

Test nr.	Speed of vessel [knots]	Duct height [m]	Water volume [m ³]	Water height PS column at $t = 0$ [m]	Water height SB column at $t = 0$ [m]
103005	0.0	0.3	10.2	0.955	-0.993
103008	15.0	0.3	10.2	0.843	-0.852

The input and output of ComFlo are of the same form as in the tests in irregular seas (see section 4.1.2). The first simulation, number 103005, is performed on a stretched grid of 200x88 grid points, which is shown in figure 4.7. Simulation 103008 is performed on two different grids, namely the same as in test 103005 and a grid of 100x44 grid points without stretching. In figure 4.8 we have given a time history of the time step for test 103008 with the 200x88 grid.

4.2.2 Results

The results of the simulations are presented in time histories of the water height in the wing tanks, the sway force and the roll moment. The agreement between the measurements and the computational results of test 103005 is good when the motion is not damped very much. As we see in figure 4.9 and 4.11 the amplitude of the water height in the port side tank and of the roll moment in the simulation is too large. Less damping is predicted than occurred in the experiment. The phase of the water height, sway force and roll moment is well predicted. In the results of test 103008 the prediction of the phase by ComFlo is less good. When the motion is damping fast the simulation gets difficulties to follow the measurements. We tried several things to make the results better.

Grid refinement A possible explanation for the deviation in the results could be that the amplitude of the damped motion was so small that it covered only 2 or 3 cells of the computational grid. Therefore we tried to make them better by changing the grid using more grid points and stretching. As can be seen from figure 4.15 refining and stretching the grid has a little influence, but the prediction of the phase and frequency has not improved much.

Turbulence As we calculate the Reynolds number, we see that the flow is turbulent (Reynolds number $Re > 10000$) but no turbulence model is built in. We simulate the flow with free slip walls which means there is no friction on the wall (see section 2.2.1). This condition does not reflect the reality, because then we have friction on the walls. In a formula this condition looks like $\mathbf{u}_t = 0$ which is called the no-slip boundary condition. Because of this condition a boundary layer is formed with thickness $\mathcal{O}(\frac{1}{\sqrt{Re}})$. In our case the Re -number in the duct is very large: $\mathcal{O}(10^4)$, so the boundary layer is thin. Because of this, many cells

are needed in the duct to simulate the boundary layer. Because the boundary layer is so thin, we do not expect much difference if we refine the grid till we can simulate the boundary layer. Because the flow is turbulent, a turbulence model could help us out. Many turbulence models are based on the concept of eddy viscosity. This concept adds viscosity to the existing viscosity to model small scale movements in the flow. In our case the viscosity used is that of water: $\nu_{water} = 10^{-6}$. To get stability of the method, upwind discretization is used. This adds a artificial diffusion which is of order 10^{-2} . We simulated experiment 103008 again with an (extra) eddy viscosity: $\nu_{eddy} = 10^{-3}$ and $\nu_{eddy} = 10^{-2}$. The results are shown in figure 4.16. We see that although the calculations are damped more, the same disagreement still occurs in the frequency and phase.

Decrease of maximal CFL-number In one oscillation period we need enough points in time where we calculate the solution. For stability, the time step must satisfy the CFL-condition. Every time step ComFlo computes the CFL-number to see if it is less than a given CFLmax (see section 3.4.3). If we want to have a smaller time step, so more points in one period, we can lower the maximal CFL-number. This is done in the simulations from which the results are shown in figure 4.17. As we see, decreasing CFLmax from 0.25 to 0.10 does not have any influence, the graphs with CFLmax of 0.25 and 0.10 are almost exactly the same. So a smaller time step does not have any influence.

The decay tests are more difficult to simulate than tests in irregular seas. Especially when the motion changes fast, the simulation has difficulties to follow the measurements. Fortunately after a little time, the simulation recovers and becomes satisfactory again. We have seen this in other simulations, for example around the 40th second in test number 103005 (see figure 4.11). There the simulation differs from the experiment, but after a short time, it is again in phase with the experiment.

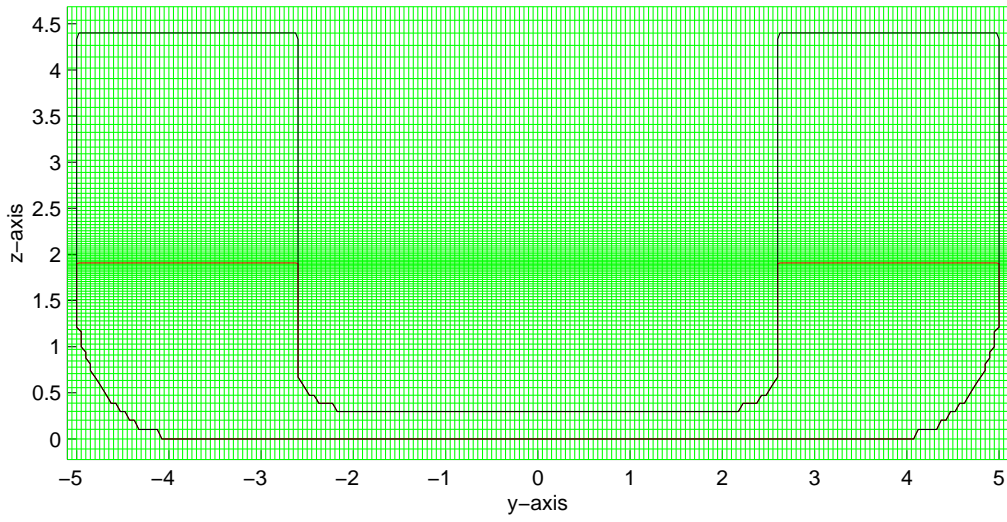


Figure 4.7: *Geometry and stretched 200x88 grid*

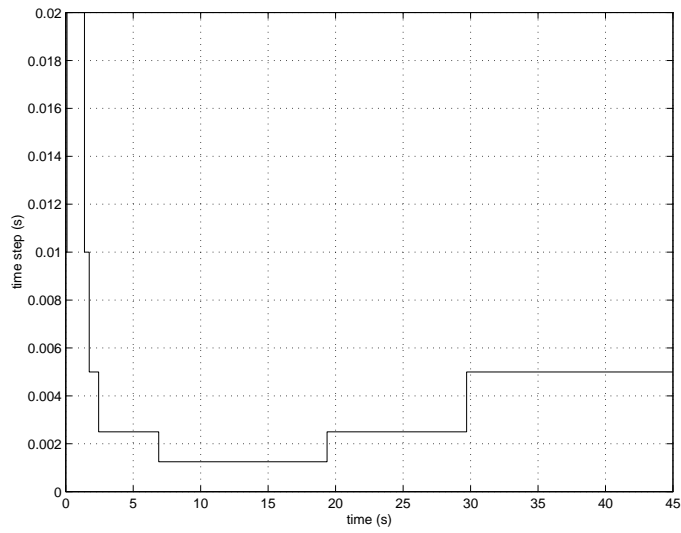


Figure 4.8: *Evolution of the time step*

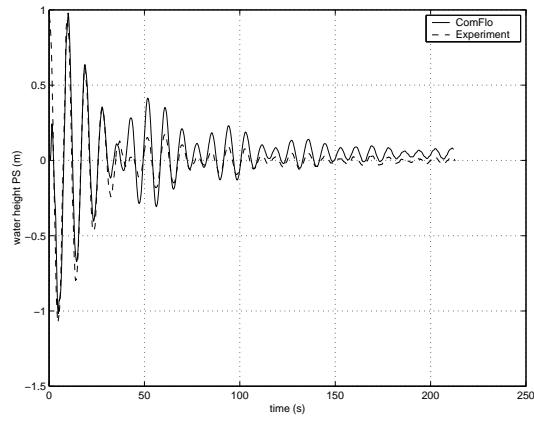


Figure 4.9: *U-tank, water height PS column, decay test 103005*

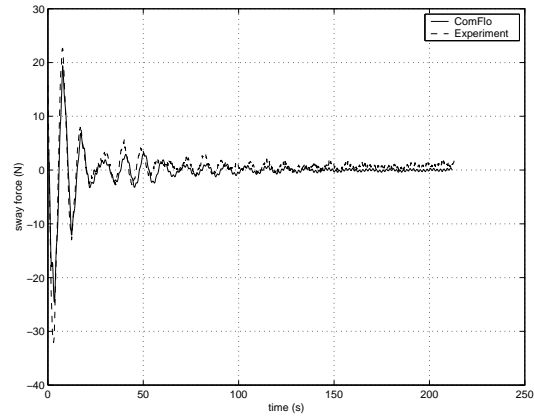


Figure 4.10: *U-tank, sway force, decay test 103005*

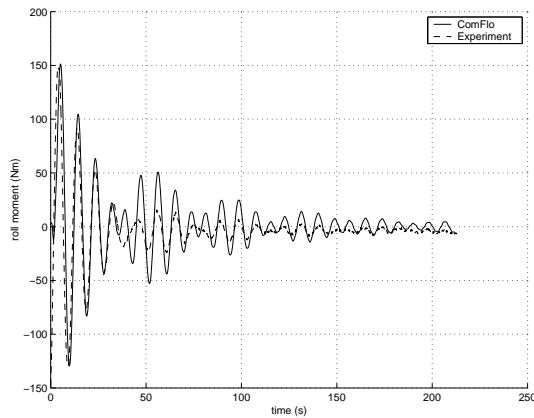


Figure 4.11: *U-tank, roll moment, decay test 103005*

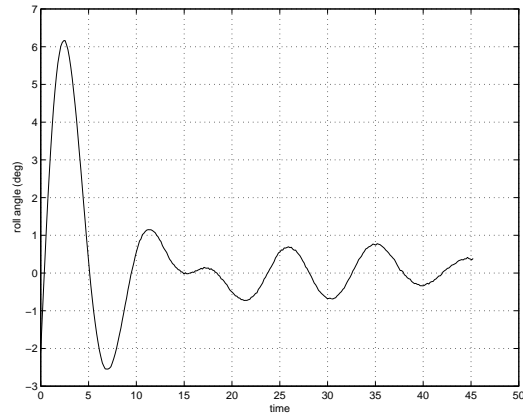


Figure 4.12: *U-tank, roll motion (input signal), decay test 103008*

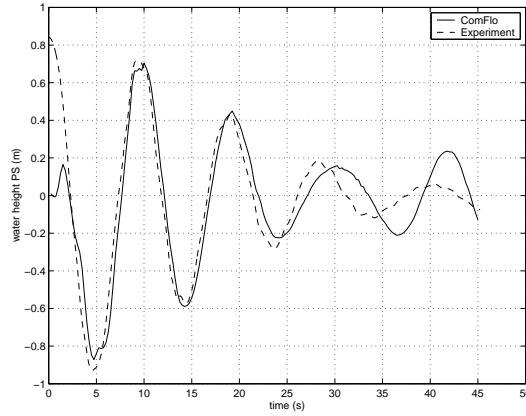


Figure 4.13: *U-tank, water height PS column, decay test 103008, grid 200x88 stretched*

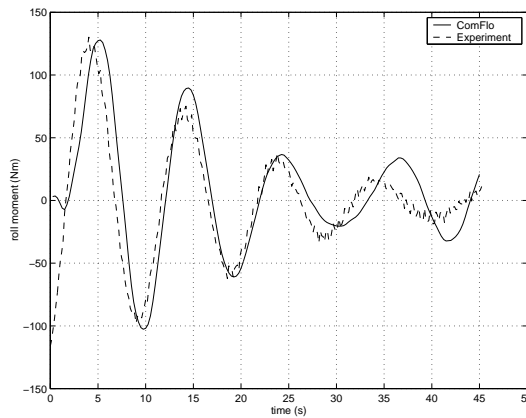


Figure 4.14: *U-tank, roll moment, decay test 103008, grid 200x88 stretched*

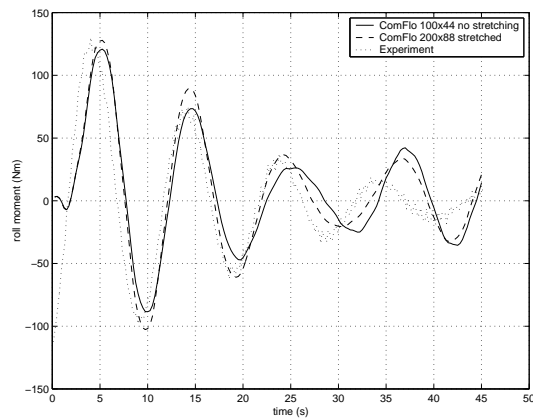


Figure 4.15: *U-tank, different grids compared, decay test 103008*

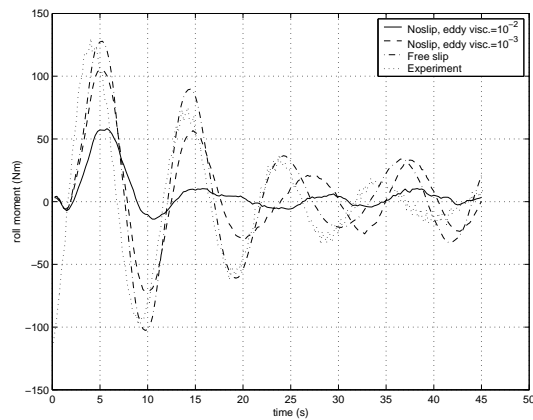


Figure 4.16: *U-tank, roll moment, free slip and no-slip with eddy viscosity compared, decay test 103008, grid 200x88 stretched*

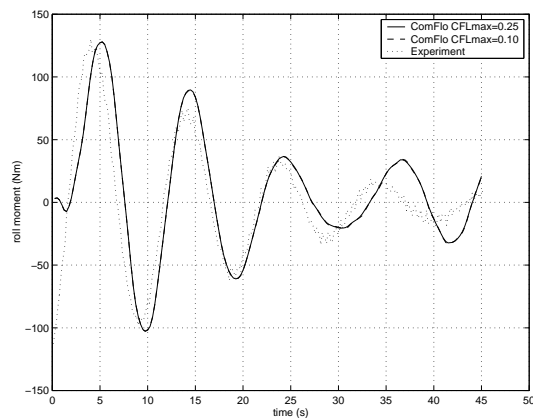


Figure 4.17: *U-tank, water height PS, different CFLmax-numbers, decay test 103008, grid 200x88 stretched*

4.3 Tests in regular seas

4.3.1 Experiment characteristics

A part of the validation of ComFlo has been done using the bench test results published by Field and Martin [5]. In these experiments a U-tank is given a forced sinusoidal oscillation. Many parameters, such as liquid level, height and length of cross-over duct and location of the tank are varied to find out the influence of the different parameters on the performance of the tank. For the validation of ComFlo only one series of tests with varying water height in the wing tanks has been used.

The tank used in the experiments has a rectangular form (see figure 4.18 for the configuration). Its dimensions are given in the table below.

	crossover duct height [m]	total width of the U-tank [m]	width of wing tanks [m]	wing tank height [m]	liquid level [m]
Test 1	0.305	12.81	2.745	3.05	0.915
Test 2	0.305	12.81	2.745	3.05	1.525
Test 3	0.305	12.81	2.745	3.05	2.135

4.3.2 Input and output of ComFlo

In these experiments, only roll motion is considered. As input in ComFlo, we prescribe the roll motion, roll velocity and roll acceleration. The roll motion is given by a sinusoidal motion with a start up time:

$$\phi(t) = A(1 - e^{-dt}) \sin(\omega t)$$

with

- A amplitude of rolling motion
- d start up parameter of rolling motion
- t time
- ω frequency of rolling motion

If we choose $d = 0.75\omega$ the start up time will be approximately equal to one period. The roll velocity and roll acceleration can be found by taking the first and second derivative of $\phi(t)$ respectively.

We are interested in the roll moment. After a set-up time the roll moment can be written as

$$M(t) = A_M \sin(\omega t + \varepsilon)$$

with

- A_M roll moment amplitude
- ε phase of roll moment

The post-processing of ComFlo gives us time histories of water height in both columns, sway and heave force and roll moment.

4.3.3 Grid distribution and time step

The simulations are performed on a grid of 100×44 grid points. The geometry and grid distribution are shown in figure 4.18. As before we give a time history of the time step for a typical simulation in figure 4.19.

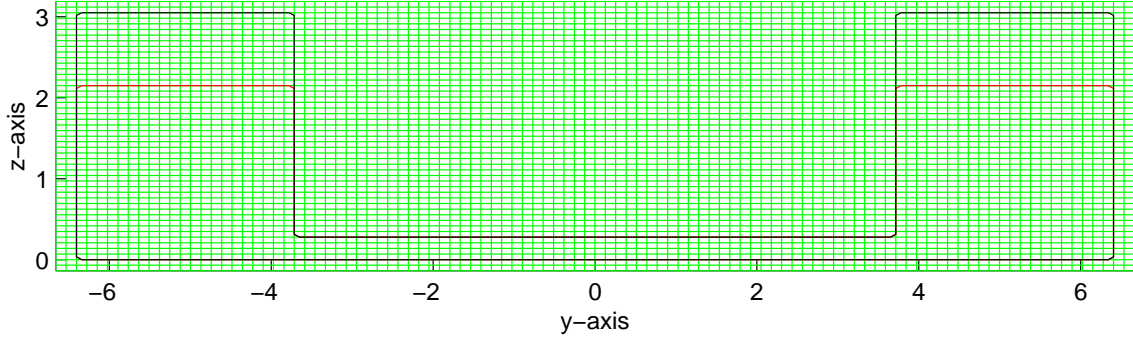


Figure 4.18: *Geometry and 100×44 grid used with the simulations*

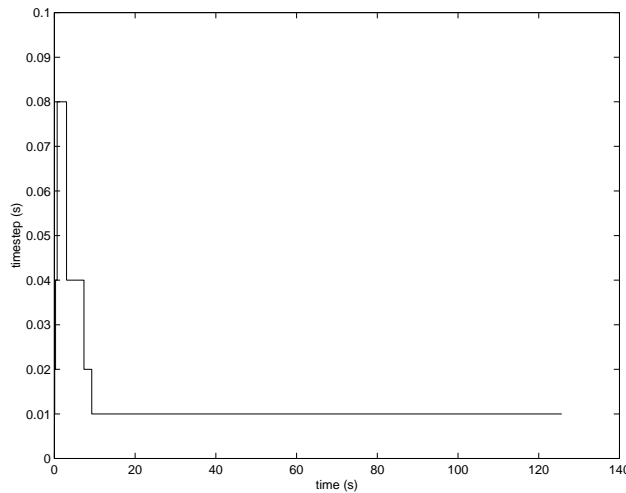


Figure 4.19: *Evolution of the time step during a typical simulation of a test in regular seas*

4.3.4 Results

This type of simulations has a start-up time before the motion of the water in the U-tank converges to periodical motion. As the frequency increases, the start-up time increases too. In figures 4.20 to 4.22 the roll motion, the calculated water height and roll moment are shown of a simulation with roll frequency of 0.4 rad/s .

The results of the simulations with various frequencies are presented in graphs containing roll moment amplitude as function of roll frequency ω and roll moment phase lag with respect to the input signal ϕ as function of roll frequency ω . In the left pictures of figures 4.23, 4.24 and 4.25, the amplitude of the roll moment is given. In the right pictures, the phase lag of the moment is given. As can be seen, the results are in good agreement with the measurements.

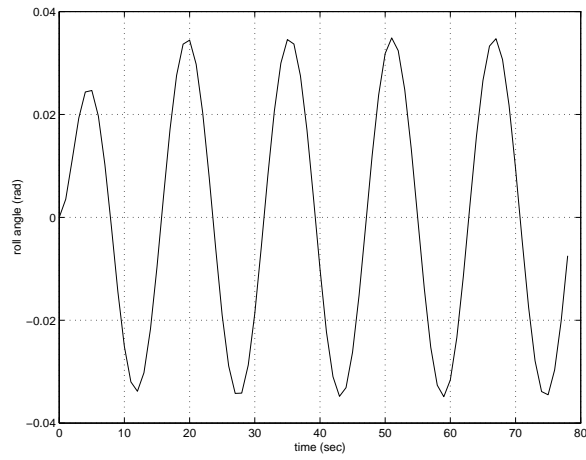


Figure 4.20: *U-tank, roll motion, roll frequency=0.4 rad/s*

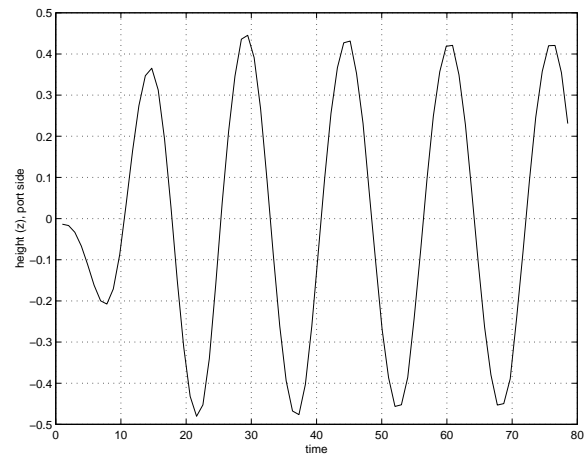


Figure 4.21: *U-tank, water height PS column, roll frequency=0.4 rad/s*

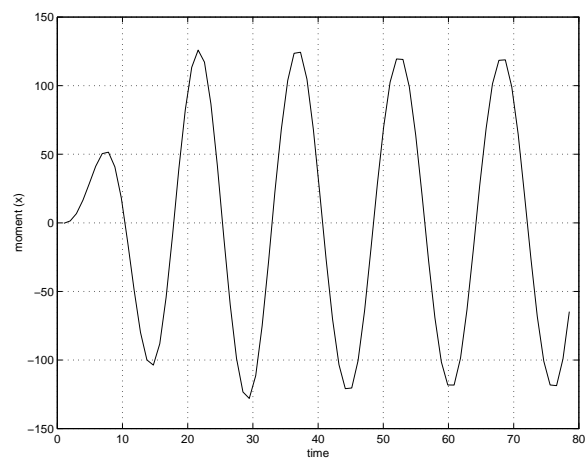


Figure 4.22: *U-tank, roll moment, roll frequency=0.4 rad/s*

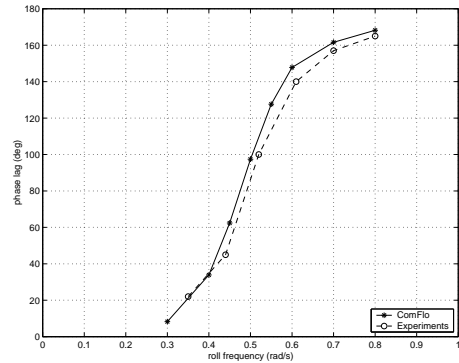
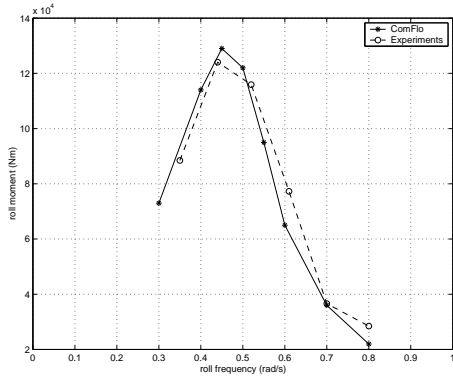


Figure 4.23: Roll moment amplitude (left) and phase lag (right) of U-tank, initial water height in both columns of 0.915 m

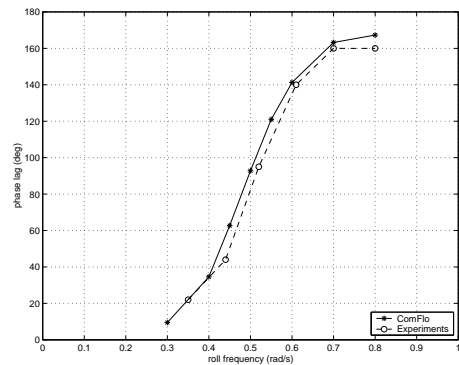
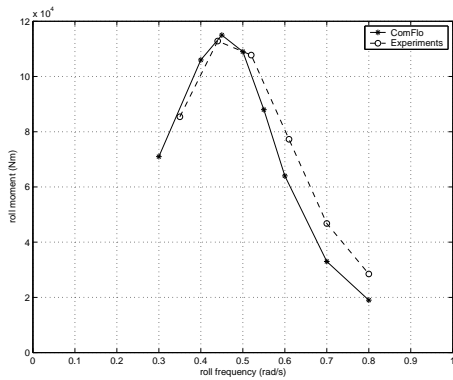


Figure 4.24: Roll moment amplitude (left) and phase lag (right) of U-tank, initial water height in both columns of 1.525 m

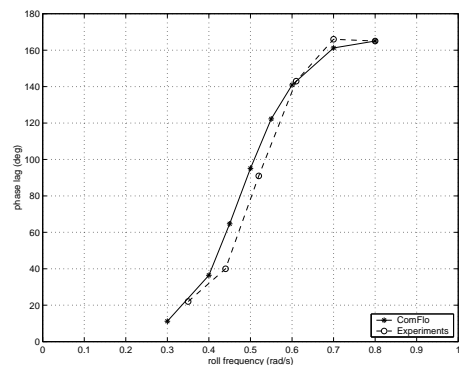
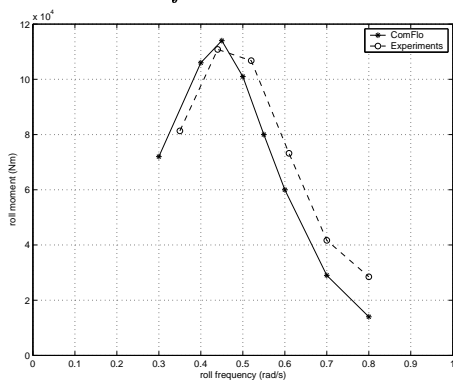


Figure 4.25: Roll moment amplitude (left) and phase lag (right) of U-tank, initial water height in both columns of 2.135 m

4.4 Conclusions about the validation

This chapter contains the results of the validation of the computer program ComFlo concerning fluid flow in a U-tubed anti-roll tank. A comparison between numerical simulations and experiments has been presented: three types of U-tank experiments have been considered. The first type were tests in irregular seas. ComFlo handles this type of problems very well. The match of the simulations of ComFlo with the measurements is very good. This is a nice result, because these experiments are a good reflection of the reality.

The results of the decay tests, where the U-tank is released after it has been given a certain amplitude are not always equally satisfying. In a few cases the simulations are less good when the U-tank is already strongly damped. We tried to make it better by refining and stretching the grid, but the results did not become better. Because the flow is turbulent we simulated a turbulence model by increasing the viscosity, but although the motion damped more, this did not have the required result. In some tests we see that the simulations recover from the problems they had earlier, so the difficulties we had do not seem to be insurmountable. The decay tests are less important in practice, but from these results we can see how ComFlo predicts the internal damping of the tank.

The last type of experiments that was used to validate ComFlo consists of tests in regular seas. Only roll motion has been considered, which is sinusoidal and small. Simulations at frequencies between 0.3 and 0.8 are done. The results are in good agreement with the experiments presented in the literature.

We can conclude that ComFlo can well be used to simulate fluid flow in U-tube anti-roll tanks. Especially in the case which is interesting from a practical view point ComFlo gives very good results.

Chapter 5

Controlled U-tanks

Stabilisation of a ship using a U-tank is optimal when the natural frequency of the U-tank is about the same as the frequency of the waves. In general, the frequency of the waves of the sea will not be the same every moment. So the U-tank does not work optimal in most cases. The tank will get better when we are able to tune the natural frequency of the tank with the roll frequency. This can be done using a control system which changes the natural frequency of the tank closer to the roll frequency.

An example of such a control system is a pump, which pumps the water in a wing tank to the other wing tank. This leads to a larger natural frequency. Another example, which has the opposite effect consists of valves in the water or air duct. If the valves are closed, they prevent the water from flowing and thus give a smaller natural frequency. We tried to simulate a control system that used valves in the air duct.

In this chapter we will first explain the physics of the control system. After that the numerical model is given and finally the results are presented and discussed.

5.1 Physics of the control system

The type of control we used is explained in an article of the company Intereng [1]. Here, an air duct is made which connects both wing tanks. This duct contains valves that can be opened and closed, depending on the motion of the tank and its water. To explain the physics of this valve-based system we will first take a closer look at the passive operation of a stabilising U-tank.

5.1.1 Passive operation

The tank operates with open valves if the roll frequency is larger than or equal to the natural frequency of the tank. We will explain the stabilising behaviour of the U-tank using figure 5.1. The tank starts with a maximum positive roll angle at (1). This means the port side wing tank is lower than the starboard wing tank. So the water is flowing with maximum velocity to the port side tank. Both tanks have about the same water level at this moment. Due to the waves of the sea, the ship starts to righten to starboard. At (3), the ship is in the upright position and the water has reached its maximum level in the port side tank. At this moment, the water in the port side tank causes the largest stabilising moment, which counteracts the wave moment.

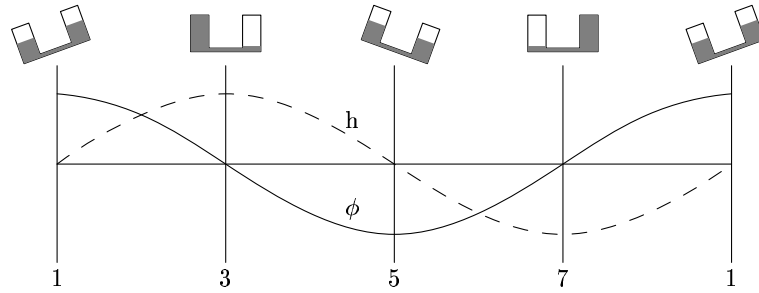


Figure 5.1: *Illustration of the behaviour of a passive U-tank*

After (3), the ship continues to roll to starboard and the water is flowing into the starboard wing tank. At (5) the ship has reached its maximum roll angle to starboard and the water level in both wing tanks is about equally high. After that the ship starts to righten and the water reaches its starboard maximum at (7). Then the water acts with maximum stabilising moment against the wave moment.

5.1.2 Controlled operation

When the roll frequency of the waves is clearly smaller than the natural frequency of the tank, the control system starts to work. Often, the control system gets its knowledge when to open or close the valves from measurements. The system is able to work very rapidly and responds to every different wave.

In figure 5.2 an illustration is given of how the water in the tank stabilises the ship in case of a smaller roll frequency than the tank's natural frequency. We have the same starting position as in the passive case. Both tanks have equal water levels and the ship has reached its maximum port side roll angle. The ship is starting to righten, but at (2) the liquid level of the port side tank has already reached its maximum although the ship is not yet upright. At this moment, the valves in the air duct are being closed, to prevent the water in the port side tank from flowing to the starboard tank. The valves are kept closed till the ship has clearly rightened and is already rolling to starboard at (4). In this way, the water is able to act with maximum stabilising moment at the right time. When the valves are opened, the water starts to flow to the starboard tank. At (5) the ship is at its maximum roll angle on starboard and the wing tanks have the same water level. Between (5) and (6), the ship starts to righten and the water is flowing into the starboard tank. Before the ship is upright, the water has reached its maximum level in the starboard tank at (6), so the valves are being closed again. They open at (8) when the ship is rolling to port side, after it has been straight up at (7). In that time, the tank water has been able to produce its maximum roll moment to stabilise the ship.

5.2 Numerical model of the control system

When we think of implementation of the control system in our computer program a few questions must be answered. In a simulation, you should first decide, whether you want to close the valves or not. Then the points in time of closing and opening the valves must be

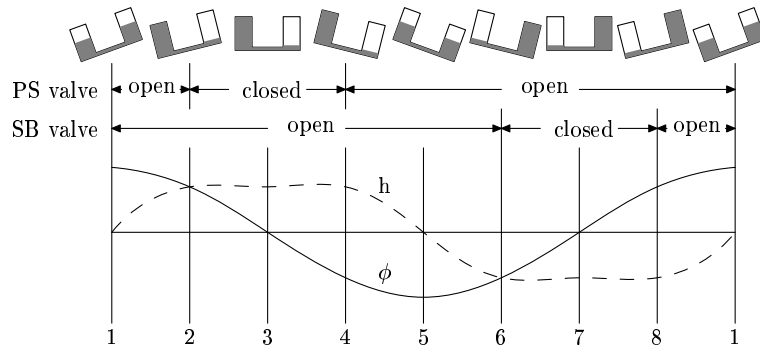


Figure 5.2: *Illustration of the behaviour of an activated U-tank*

determined. Finally, a way to hold the water a few moments at one level must be found. In this section, these problems are solved.

5.2.1 Making the decision to close the valves

The valves-based control system works on the principle of artificially lowering of the natural frequency of the U-tank. The tank stabilises optimal when the roll frequency is almost equal to the tank's natural frequency. So we should switch control on, if the natural frequency of the tank is larger than the roll frequency.

We assume that the natural frequency of the tank is known in advance. The roll frequency must be determined during the simulation. If we have a simulation in regular seas, the roll frequency has a constant value and is known in advance.

When the ship undergoes irregular seas, every wave has a different roll frequency. This frequency must be determined during the simulation, every wave again. We can do this by clocking the time between the moment that the roll angle is zero and the moment that the roll angle has reached its maximum. If we multiply this time interval by four, we find the approximate period of this wave. Then you are right on time to close the valves, when the water reaches its maximum level in one of the wing tanks soon after this.

5.2.2 Determination of the closing time of the valves

When it has been decided that the valves will be closed during a certain wave, the point in time of closing the valves must be determined. We have seen in section 5.1.2 that this moment is marked by a maximum water level in one of the wing tanks. This moment can be found easily, by keeping track of the water volume of the wing tanks. If the volume is maximal, than the water height will be maximal too.

5.2.3 Simulation of the closed valves

If the valves in the air duct are closed, the water level will fall a little and then oscillate to an equilibrium because of the compressibility of air. The air in a wing tank satisfies the gas law (we assume air to be an ideal gas)

$$\frac{p V}{T} = n R$$

with

- p the pressure;
- V the volume of the gas;
- T the gas temperature;
- n the number of particles;
- R the gas constant.

We assume that the temperature will be constant. Because n and R are constants too, the gas law turns into

$$p V = \text{constant}.$$

To simulate the changing pressure in the air in the top of the wing tanks, we should adapt the pressure at the free surface with an amount that we can calculate using the gas law. Let t_c be the point in time when the valves are closed. Then, the pressure is equal to the atmospheric pressure p_0 and the air volume is equal to V_c . A little time later, when the valves are still closed (time t_{n+1}), the gas law leads us to

$$p_{n+1} V_{n+1} = p_0 V_c.$$

So the pressure at the free surface at time t_{n+1} becomes

$$p_{n+1} = p_0 \frac{V_c}{V_{n+1}}.$$

5.2.4 Opening the valves

Finally, we have to know when we want to open the valves again, so that the water can flow to the other wing tank. In section 5.1.2 we have seen that the valves should be opened when the ship is clearly rightening. But this is too vague to implement.

Our goal is to lengthen the natural period of the tank to the roll period of the wave. If the closed valves were able to keep the water at the same level (which is not possible in reality because of the compressibility of air) we can calculate the optimal closing time period as follows. At the moment the valves are closed, the ship has a certain roll velocity $\dot{\phi}_x(t_{close})$ (in figure 5.2 at stage 2). The ship's roll velocity will get larger until the roll angle is zero at stage 3. Around this point in time the ship rolls with maximum roll velocity ($\dot{\phi}_{x_{max}}$). After that the velocity decreases and will reach the value $\dot{\phi}_x(t_{close})$ again (at stage 4). At this point in time we should open the valves if the same water level was maintained. We can calculate this $\dot{\phi}_x(t_{close})$ when we presume regular seas given by

$$\phi_x(t) = A \sin(\omega t),$$

with A the amplitude and ω the roll frequency. The closing time period is given by

$$\Delta t_{optimal} = \frac{1}{2} \left(\frac{2\pi}{\omega} - \frac{2\pi}{\omega_{nat}} \right), \quad (5.1)$$

where ω and ω_{nat} denote the roll frequency and the tank's natural frequency respectively. Now the roll velocity at the opening and closing time point can be calculated as

$$\begin{aligned}\dot{\phi}_x(t_{close}) &= \dot{\phi}_x(t_{roll=0} - \frac{1}{2}\Delta t_{optimal}) \\ &= A\omega \cos(\frac{1}{2}\pi (1 - \frac{\omega}{\omega_{nat}})).\end{aligned}\tag{5.2}$$

In reality, the water level has dropped a little, so we expect the valves should be closed somewhat longer than the optimal closing period we calculated above. Here, we neglect this and use 5.1 and 5.2 to determine the opening time point. The roll velocity we calculated is a factor of the maximal roll velocity $A\omega$. This factor is equal to $\cos(\frac{1}{2}\pi (1 - \frac{\omega}{\omega_{nat}}))$. Now the valves are opened if the roll velocity satisfies

$$\dot{\phi}_x(t_{open}) = \cos(\frac{1}{2}\pi (1 - \frac{\omega}{\omega_{nat}}))\dot{\phi}_{x_{max}}.$$

It would have been much easier if we simply could prescribe the time period $\Delta t_{optimal}$ as the closing period. But then a problem occurs when the tank is in irregular seas. If the opening point in time is prescribed by $t_{open} = t_{close} + \Delta t_{optimal}$ it is possible that the valves are opened after the ship has reached the maximum roll angle at the other side. This is because in irregular seas the roll frequency is not known in advance. The same problem occurs if the opening time point is prescribed using the roll motion. But when using a factor of the maximum roll velocity, it is guaranteed the valves are opened in the period after the rightening of the ship (with roll velocity is maximal) and before it reaches its maximum roll angle at the other side (with roll velocity zero). In this way we succeed to lengthen the tank's natural period.

5.3 Results

We will show results of two series of simulations in regular seas. In the first series, we simulate the water in a U-tank where the valves of the control system are closed for several fixed time periods Δt . From this we can see the effect of the closing period on the roll moment. Then we will present results from simulations of a U-tank with a control system with closing time period as described above in section 5.2.4.

In Appendix A, snapshots of the velocity field from a simulation of an activated tank in regular seas are given. We see there, that the water is kept blocked for a few seconds very well.

5.3.1 Valves closed for a fixed period of time

The purpose of these simulations is to see the effect of the closing period on the roll moment and to determine the period of time of closed valves, that gives the largest stabilising roll moment. We have seen we can calculate an optimal closing period if we assume the water will be held on the same level perfectly and we will compare this with the closing time in the simulation. We took the same U-tank as the one which was used for the validation (see figure 4.1). The natural frequency of this tank is about 0.6 rad/s. At several roll frequencies of regular seas, varying from 0.3 to 0.6 rad/s, we simulated the water motion in the tank. When the water reached the maximum water height in one of the wing tanks, the valves were closed

for a certain time period Δt , where Δt was varied from 0 to 4.0 seconds. The simulations are done on a grid of 50x22 grid points, the roll amplitude is set to 0.0849 rad. The results are shown in figure 5.3, where the roll moment is given as a function of the closing period Δt

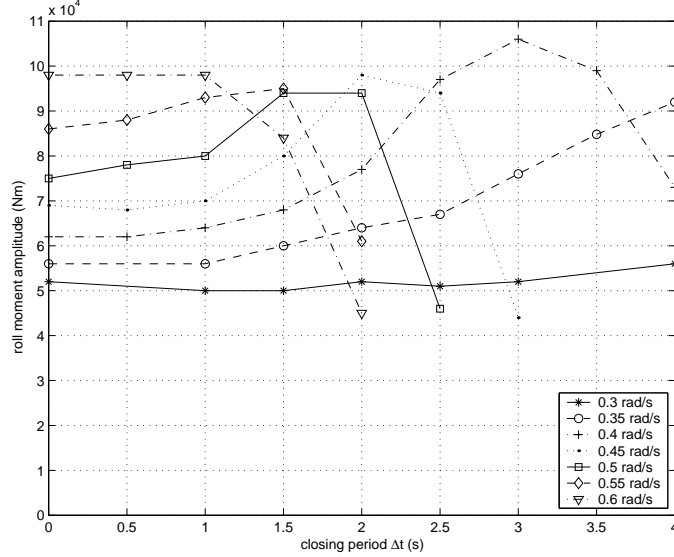


Figure 5.3: *Roll moment as function of closing period Δt for various frequencies*

From this figure we find that at a roll frequency of 0.6 rad/s the roll moment stays the same if we close the valves 0, 0.5 or 1.0 second. So the valves do not have to be closed to maintain the same roll moment. If the valves are closed for more than 1.0 second, the roll moment decreases. This result is what we expected, because the natural frequency of the tank is about 0.6 rad/s and then the tank works optimal.

When the roll frequency is smaller than the tank's natural frequency, we should close the valves for a certain period of time. This closing period depends on the roll frequency. In the previous section we determined the optimal closing period if the water level did not fall in the closing period. Using that the natural period of the tank is equal to 10.5 s we get

$$\Delta t_{optimal} = \frac{1}{2} \left(\frac{2\pi}{\omega} - 10.5 \right), \quad (5.3)$$

where ω denotes the roll frequency of the waves. In practice we expect that we should close the valves a little longer because the water loses some height due to the compressibility of air.

Let us check this for a roll frequency of 0.4 rad/s. Theoretically, the optimal closing period given by equation 5.3 equals $\frac{1}{2}(15.7 - 10.5) = 2.6$ seconds. If we look in figure 5.3 we see that the largest roll moment amplitude occurs at a Δt of 3.0 seconds which is a little larger than the period the formula gave us. This is in agreement with what we expected.

If we compare our figure with figure 25 from the report of Stigter [11], we see that closing the valves has the same effect, namely a larger roll moment, as making the duct connecting the wing tanks longer. This is consistent, because both actions, lengthening the duct and closing the valves, result in a smaller natural tank frequency.

5.3.2 Stabilisation with the valves-based control system

Simulations were performed of a U-tank that was equipped with the control system described in section 5.2. We simulated the motion of the water in the activated U-tank in regular seas with several roll frequencies. The same simulations were performed with a passive tank to see the influence of the control system. In figures 5.4 and 5.5 the water volume in the port side wing tank and the roll moment are shown of a U-tank in seas with a roll frequency of 0.3 rad/s. If the water is blocked by closing the valves, we see that the water level drops a bit and starts to oscillate. This oscillatory motion of the water causes the big wiggle in the roll moment as shown in figure 5.5. Here we see that the roll moment increases a lot when the control is active.

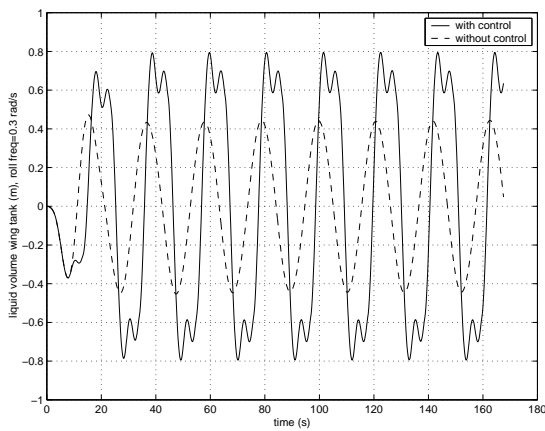


Figure 5.4: *Water volume in port side tank of an activated U-tank*

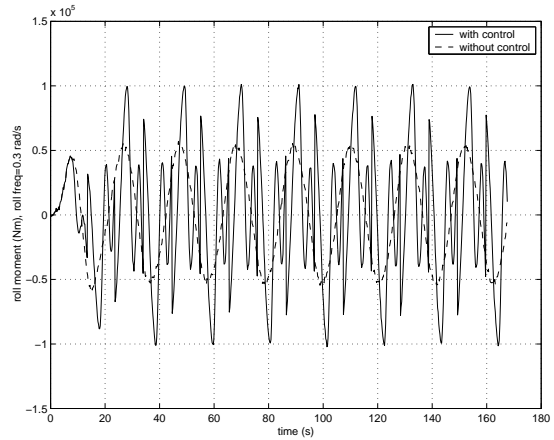


Figure 5.5: *Roll moment of the water in an activated U-tank*

In figure 5.6 the amplitude of the roll moment is given as a function of the roll frequency. In the case of the passive tank, the amplitude of the roll moment has a maximum at about 0.6 rad/s which is the natural frequency of the tank. Looking at the results of the activated tank, we see that for frequencies smaller than the natural frequency, the moment is increased significantly by imposing active control.

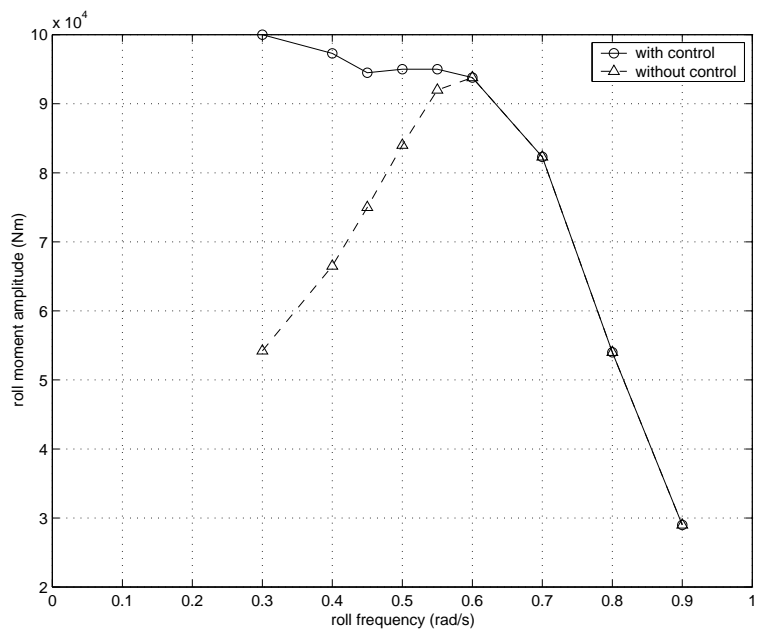


Figure 5.6: *Amplitude of the roll moment of passive versus activated U-tank*

Chapter 6

Coupling with a linear two dimensional ship motion model

Until now, we have only looked at the influence of the tank motion on the water. The results gave us the forces and roll moment in return induced by the water on the tank. We come much closer to reality if we couple the results from ComFlo to a ship motion model. Then we have the interaction of the ship motion due to the waves and the motion of the water in the anti-roll U-tank. We have chosen a linear 2DOF ship motion model, which describes the sway and roll motions of the ship.

6.1 Linear 2DOF ship motion model

The differential equations that describe the sway and roll motion of a ship are given by

$$(M + A_{22}) \ddot{y} + B_{22} \dot{y} + C_{22} y + A_{24} \ddot{\phi} + B_{24} \dot{\phi} + C_{24} \phi = F_y^{wave} + F_y^{tank} \quad (6.1)$$

$$(I_{xx} + A_{44}) \ddot{\phi} + B_{44} \dot{\phi} + C_{44} \phi + A_{42} \ddot{y} + B_{42} \dot{y} + C_{42} y = M_x^{wave} + M_x^{tank} \quad (6.2)$$

with

- y the sway motion;
- ϕ the roll angle;
- M the mass of the ship;
- I_{xx} the ship's moment of inertia about the x -axis;
- A_{ij} added mass coefficients;
- B_{ij} damping coefficients;
- C_{ij} restoring coefficients;
- F_y^{wave} and M_x^{wave} the wave excitation force and moment respectively;
- F_y^{tank} and M_x^{tank} the tank excitation force and moment respectively;

The mass M and moment of inertia I_{xx} of the ship and restoring coefficients are known in advance. The wave excitation terms are given by a time series of a sinusoidal function. By solving the Navier-Stokes equations, the tank excitation force and roll moment are determined. The added mass and damping coefficients depend on the oscillation frequency ω . The added mass and damping contributions can be expressed in the associated retardation functions K_{ij} :

$$K_{ij}(t) = \frac{2}{\pi} \int_0^\infty (B_{ij}(\omega) - B_{ij}^\infty) \cos(\omega t) d\omega \quad i, j = 2, 4 \quad (6.3)$$

with B_{ij}^∞ damping coefficients at infinite frequency.

The radiation sway force and roll moment are expressed as a convolution integral involving the time history of the ship's velocities:

$$F_y^{rad}(t) = -B_{22}^\infty \dot{y} - \int_0^t K_{22}(t-\tau) \dot{y}(\tau) d\tau - B_{24}^\infty \dot{\phi} - \int_0^t K_{24}(t-\tau) \dot{\phi}(\tau) d\tau \quad (6.4)$$

$$M_x^{rad}(t) = -B_{44}^\infty \dot{\phi} - \int_0^t K_{44}(t-\tau) \dot{\phi}(\tau) d\tau - B_{42}^\infty \dot{y} - \int_0^t K_{42}(t-\tau) \dot{y}(\tau) d\tau \quad (6.5)$$

The retardation functions are known in advance and given by time series. In figure 6.1 the retardation function K_{44} (roll into roll) which is used in the calculations is shown.

Using the retardation functions, the coupled set of differential equations is written as:

$$(M + A_{22}^\infty) \ddot{y} + A_{24}^\infty \ddot{\phi} = F_y^{wave} + F_y^{rad} + F_y^{tank} - C_{22} y - C_{24} \phi \quad (6.6)$$

$$(I_{xx} + A_{44}^\infty) \ddot{\phi} + A_{42}^\infty \ddot{y} = M_x^{wave} + M_x^{rad} + M_x^{tank} - C_{44} \phi - C_{42} y \quad (6.7)$$

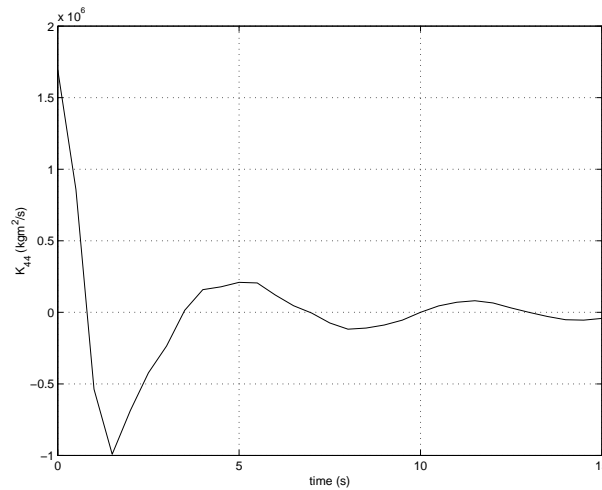


Figure 6.1: Retardation function roll into roll

6.2 Numerical model of 2DOF ship motion model

The tank motion and the water motion in the tank are divided into two different systems. First we solve the Navier-Stokes equations for the motion of the water in the tank as explained in chapter 3 of the report. This water motion is input for the ship motion model in the terms F^{tank} and M^{tank} . For the calculation of F^{tank} and M^{tank} we follow the idea of Gerrits and Veldman as explained in [8]. This idea is based on writing the forces and moments which are induced by the water flow in the tank, in terms of accelerations.

When we compare the model of [8] with our linear 2DOF ship motion model, the force and moment induced by the tank water in terms of acceleration are given by:

$$\mathbf{F}^{tank} = - \int_V \rho \left(\frac{D\mathbf{u}}{Dt} + 2\boldsymbol{\omega} \times \mathbf{u} + \mathbf{F}_g \right) dV \quad (6.8)$$

$$\mathbf{M}^{tank} = - \int_V \rho \mathbf{r} \times \left(\frac{D\mathbf{u}}{Dt} + 2\boldsymbol{\omega} \times \mathbf{u} + \mathbf{F}_g \right) dV \quad (6.9)$$

where \mathbf{r} denotes the center of mass of the coupled system, and \mathbf{F}_g the gravity force. From these vectors we take the second and first component respectively to get F_y^{tank} and M_x^{tank} .

The time discretization of equations 6.6 and 6.7 is straightforward. If we call the right-hand side of the equations 6.6 and 6.7 \mathcal{L}_y and \mathcal{A}_x respectively, we discretize the variables on the following level:

$$(M + A_{22}^\infty) \ddot{y}^{n+1} + A_{24}^\infty \ddot{\phi}^{n+1} = \mathcal{L}_y^n \quad (6.10)$$

$$(I_{xx} + A_{44}^\infty) \ddot{\phi}^{n+1} + A_{42}^\infty \ddot{y}^{n+1} = \mathcal{A}_x^n \quad (6.11)$$

First the right-hand side of equations 6.10 and 6.11 is calculated. For the tank excitation terms, that consist of an integral over the volume, the VOF-function can be used. After this, \ddot{y}^{n+1} and $\ddot{\phi}^{n+1}$ are determined using Gauss elimination. These quantities are then integrated to \dot{y} and $\dot{\phi}$ by the fourth-order Runge Kutta method. The next integration to ϕ and y is performed using the Forward Euler method, which is accurate enough because these quantities are primarily needed for the post-processing.

6.3 Results

To show the stabilising effect of the U-tank, we performed simulations of the motion of a ship with and without U-tank. We used the above model for the interaction between the motion of the fluid and the ship motion. Making these results we only considered roll motion, so we solved equation 6.7. The wave excitation moment was given by a simple sine function, with a little start-up time:

$$M_x^{wave} = -A (1 - e^{-dt}) \sin(\omega t)$$

where A denotes the amplitude of the excitation, given in input file `shipmo.in` as `AM4` (see Appendix B.4), d is a start-up parameter and ω denotes the wave excitation frequency (in `shipmo.in` given by `rollfrq`). The dimensions of the U-tank are given in figure 4.1 and the ship parameters in table 6.1. All these parameters can be put in the input file `comflo.in`.

First we will show the results for one particular excitation frequency where the excitation moment amplitude was $97 \cdot 10^3$ Nm. Later on results for various frequencies with much bigger

Mass	$1.0225 \cdot 10^6 \text{ kg}$
Center of mass	3.1 m above bottom U-tank
Moment of inertia xx	$17525.7 \cdot 10^3 \text{ kg m}^2$
Moment of inertia yy	$196143.8 \cdot 10^3 \text{ kg m}^2$
Moment of inertia zz	$189126.7 \cdot 10^3 \text{ kg m}^2$

Table 6.1: Parameters of the ship used in the simulations

excitation moment amplitude of $500 \cdot 10^3 \text{ Nm}$ are presented. All simulations were performed on a grid of 100x44 grid points.

6.3.1 Excitation frequency near tank resonance

In figure 6.2 the roll angle of the ship with an excitation frequency of 0.6 rad/s is shown. The dashed line denotes the roll angle of the ship without water in the U-tank, so without the stabilising effect whereas the solid line is the roll angle with stabilising tank water. We see that the U-tank has a large stabilising effect, the roll reduction is about 40 %.

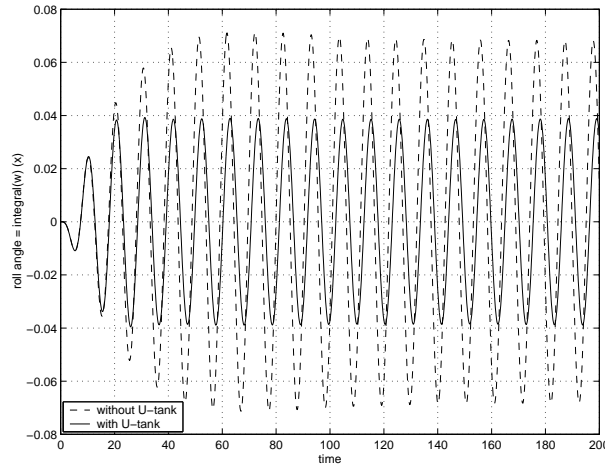


Figure 6.2: *Ship's roll angle, with and without stabilising tank*

In equation 6.7 we see that there are a few different types of moment which influence the roll motion of the ship. If we go through the equation from left to right we have the moment caused by the wave, or the excitation moment. M_x^{rad} denotes a moment induced by the motion of the ship in the sea, a damping term. The fluid in the tank accounts for the moment denoted by M_x^{tank} . The last two terms are restoring moments due to the motion of the ship in the sea.

In figure 6.3 the right-hand-side of equation 6.7 is split in the above mentioned contributions. The left-hand figure shows the contributions in the first 100 seconds of a simulation without U-tank with a excitation frequency of 0.6 rad/s. The same for the right-hand figure, but with U-tank.

In both cases we see that the restoring moment is very large in comparison with the other moments. In the left hand figure, the tank moment is zero, because there is no tank. The

damping contribution counteracts the excitation as can be expected.

In the case with stabilising U-tank, the radiation moment and tank moment counteract the excitation. We can conclude that the U-tank works very well in the case of an excitation frequency of 0.6 rad/s.

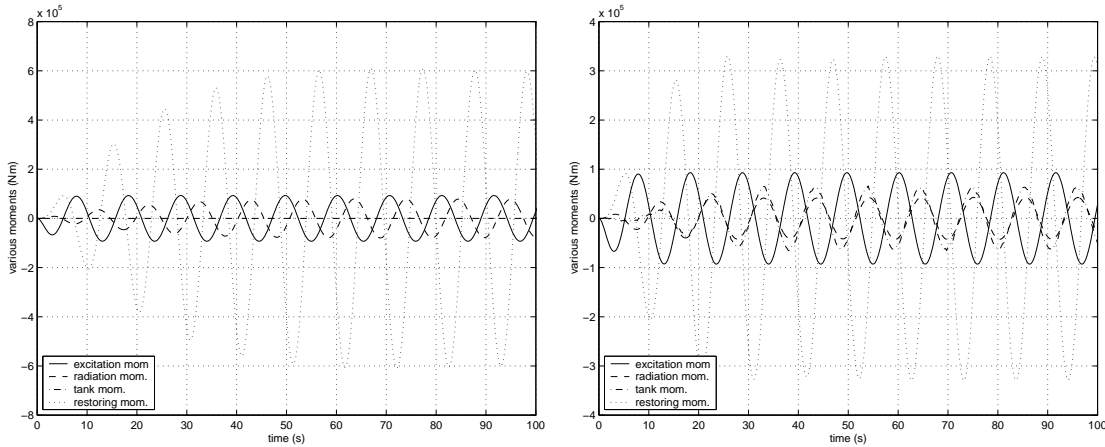


Figure 6.3: *Contribution of various moments; left: without U-tank, right: with U-tank*

6.3.2 Various frequencies: no tank, passive tank and activated tank

Finally simulations of coupled ship and tank motion are done in a frequency range of 0.3 to 0.8 rad/s with excitation amplitude of $500 \cdot 10^3$ Nm. This excitation takes care of a large roll angle at ship's resonance.

Three different configurations are used: ship without tank (or: no water in the tank), ship with passive tank and ship with activated tank. In figure 6.4 a time history of the roll angle of a simulation with excitation frequency 0.45 rad/s is shown. It can be seen that the roll angle is increased when the ship is stabilised by a passive tank. When the tank is controlled, the roll angle decreases again till the roll angle of the unstabilised ship.

In figure 6.5 the roll angle of a ship without tank and with passive and activated tank is shown as function of the excitation frequency. In the case of an unstabilised ship, we see that the ship gets its largest roll amplitude at frequencies near the ship's natural frequency which is about 0.6 rad/s. When we put a passive tank in the ship, the tank damps the roll motion of the ship at frequencies near the tank's natural frequency. At the frequency of 0.6 rad/s the tank accounts for about 25% roll reduction. If we look at frequencies not too close to the resonance frequency, we see that the passive tank does not stabilise anymore, it even increases the roll angle of the ship. This is why most U-tanks have a control system. If we switch control on, we see that at frequencies below the resonance frequency, the control system takes care of reduction of the roll angle to about the roll angle of the unstabilised ship.

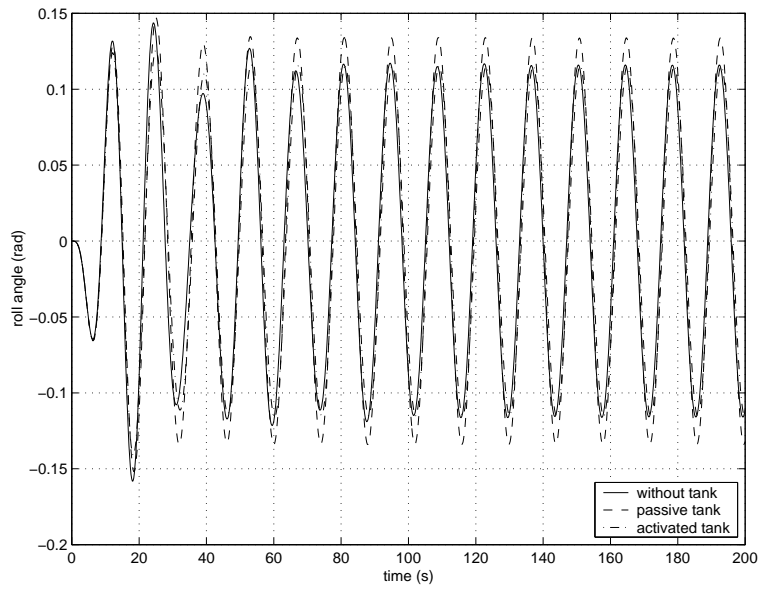


Figure 6.4: *Roll angle of ship in seas with excitation frequency of 0.45 rad/s*

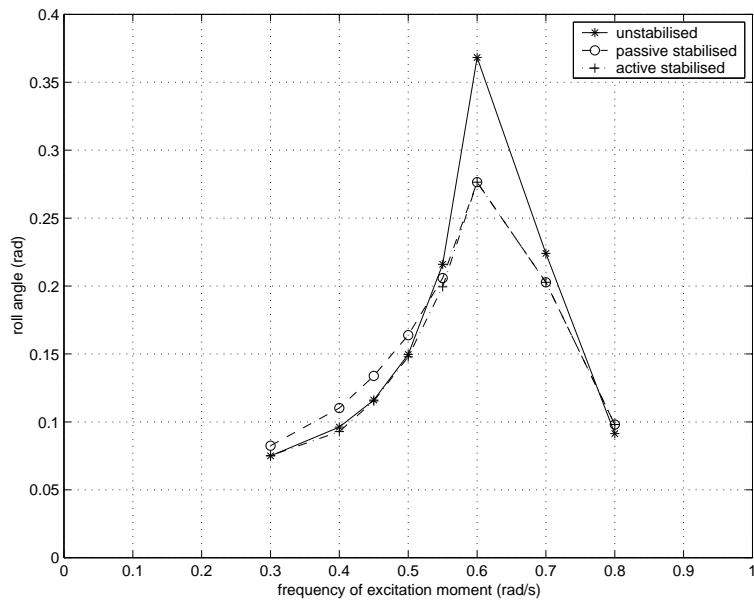


Figure 6.5: *Roll angle amplitude of a ship without tank, with passive and with activated tank*

Chapter 7

Conclusions

This report contains results of computer simulations of fluid flow in a ship stabilising U-tank. First the computer program ComFlo was validated for its use in simulation of the water in the tank with prescribed tank motion. This was done using experiments in irregular waves and decay tests, both performed by Marin, and using experiments in regular seas from an article of Field and Martin ([5]). Specific conclusions can be found at the end of chapter 4 which handles the validation of ComFlo. The general conclusion of this work is that ComFlo is very suitable for this purpose. Most of the results gave a good representation of the experiments. In the simulations of the decay tests, some problems were found when the tank was strongly damped. The solution to this problem may be found in considering the boundary layers. Therefore the tank walls should be made no-slip, and a very fine grid is needed to catch the boundary layer.

A U-tank only stabilises the ship in a small frequency range. There is one frequency where the tank works optimal. For other frequencies the tank loses its stabilising effect, and for some frequencies smaller than the optimal frequency, it even increases the roll angle of the ship. For this purpose control systems are built, so that the tank is effective in a larger frequency range. In ComFlo a control system based on valves in the air duct which connects both wing tanks is built in. This system works for wave frequencies smaller than the natural tank's frequency. The results show that the control system works very well. The roll moment produced by the water in the U-tank which counteracts the moment exerted by the sea increases much and thus has a stabilising effect.

To see the actual effect of the U-tank on the roll angle of a ship we must have a full coupling between the fluid motion in the tank and the motion of the ship. In this report a linear ship motion model has been chosen. The results show that the U-tank has much effect on the motion of the ship. Near its optimal frequency, the tank reduces the roll motion of the ship. For smaller frequencies the tank has no effect or even increases the roll motion. When we switch on the control system, the activated tank reduces the motion again, which shows us the usefulness of the control system. The ship motion model was implemented for sway and roll motion, but only the roll motion was tested. In the future, the coupling can be extended to full coupling, first in 2 dimensions, then in all 6 degrees of freedom.

In this report we have seen that ComFlo can simulate fluid motion in a passive and acti-

vated U-tank very well. Furthermore a start has been made with simulations of the motion of a ship, equipped with a U-tank. The results gave us confidence in the methods used. Still, much work can be done in the future. First of all, the flow simulations and the validation where the full motion of the ship is prescribed, can be extended to three dimensions. More attention can be given to the decay tests where some problems that occurred in the validation are still unsolved. Furthermore, the numerical model of the control system based on valves can be refined and other control systems can be simulated. Therefore more details of the operation of a control system in practice should be examined and added to ComFlo. The final goal is to simulate arbitrary ship motion where the ship is equipped with an anti-roll tank. Therefore we need a full coupling of the water flow in the anti-roll tank and the ship motion. The results shown in this report make us believe this is not too far away.

Appendix A

Snapshots

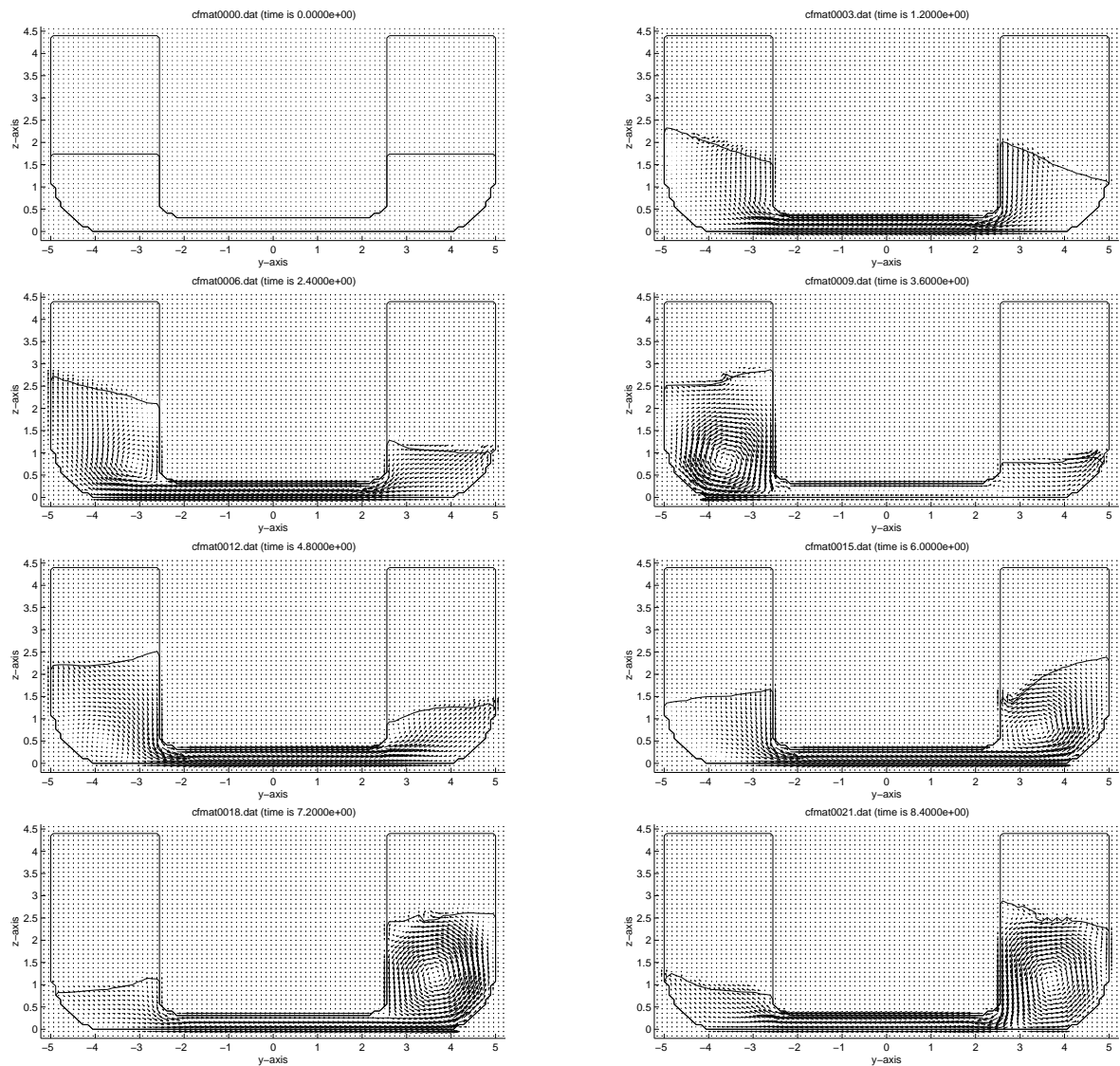


Figure A.1: Velocity field of a simulation in irregular seas, $t=0.0$ to 8.4 seconds

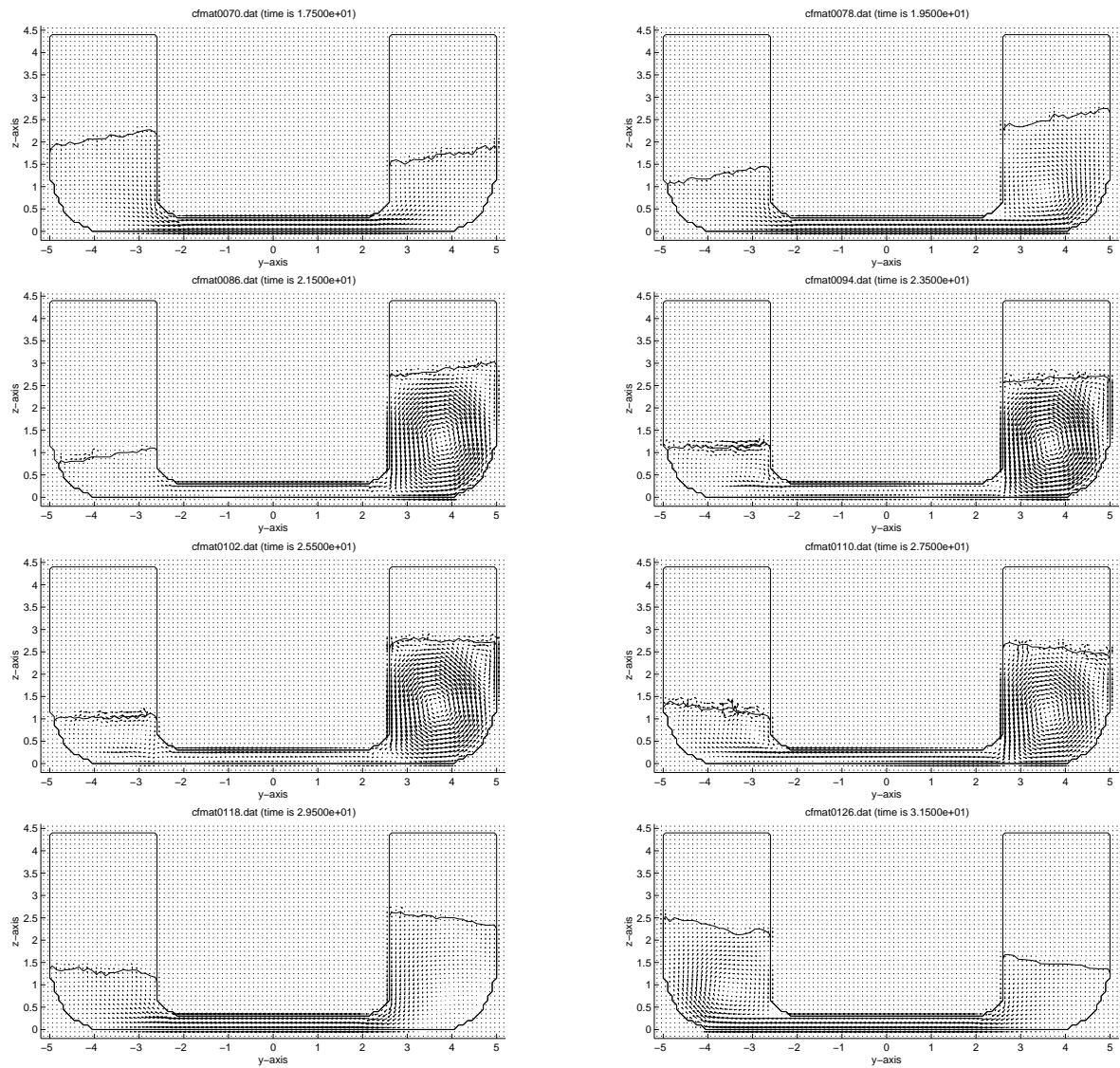


Figure A.2: Velocity field of a simulation with activated tank, valves closed from $t=21.29$ to 28.65 seconds, snapshots from $t=17.5$ to 31.5 seconds

Appendix B

Program Description

B.1 Calling sequence

ComFlo consists of several subroutines, that are called in the following order:

Setup	SETPAR	GRID	
	SETCSA		
	BNDLAB	BNDDEF	
		IOLAB	
	SETFLD	SURDEF	
		SURLAB	
		BC	IOBC VELBC
Time integration	LIQWTS		
	INIT	FLUXBC	
	TILDE	BDYFRC	TRAFOS
	SOLVEP	COEFL	
		COEFR	
		PRESBC	
		PRESIT	SLAG
		VELBC	
		TUMBLE	
		VFCONV	SURLAB
		BC	IOBC VELBC DTADJ

After the time integration, several subroutines are called for post-processing reasons.

B.2 Subroutines

In this section a short description is given of the subroutines in ComFlo.

AUTOSV : Creates and reads autosave files that are used for restarts.
AVS : Post-processing: produces data for the use of AVS.
BC : Computes the boundary velocities.
BDYFRC : Computes translation and rotation in virtual body force. Determines the roll frequency for control reasons.
BNDDEF : Defines the boundary of the geometry.
BNDLAB : Calculates apertures, and labels the cells and velocities, based on the geometry.
CELLNR : Computes indices of the vertex of a point with given co-ordinates.
COEFL : Calculates the left hand side of the pressure Poisson equation.
COEFR : Calculates the right hand side of the pressure Poisson equation.
COM : Computes the center of mass of the fluid.
CROSS : Returns the cross product of two vectors.
DTADJ : Adapts the time step using the CFL-condition.
FILLBX : Post-processing: Returns data about the volume of fluid in a certain box.
FLUXBC : Computes **BB** and **FB** flux velocities.
FLUXBX : Post-processing: Returns data about the fluxes through a certain box.
FRCBX : Post-processing: Returns data about the forces and moments in a certain box.
GRID : Generates a (stretched) grid.
INIT : Initialises variables for a new time step.
INTERP : Interpolates between values of variables.
IOBC : Creates boundary conditions at input and output boundaries.
IOLAB : Creates input and output labels.
LIQPCT : Computes liquid percentage and returns it to screen.
LIQWTS : Computes liquid volume in the wing tanks for control reasons.
MATLAB : Post-processing: produces data for the use of Matlab.
MNTR : Post-processing: monitoring of pressure or velocity in a fixed point.
MOI : Computes the moments of inertia of the fluid.
NEIGHB : Determines the neighbours of a certain cell.
NORMAL : Computes the normal of a solid boundary.
PRESBC : Resets the pressure in the **BS**, **BE** and **E**-cells to p_0 . Computes the pressure in the **S**-cells using interpolation. Changes the pressure at the free surface to block the water if control of U-tank is on.
PRESIT : Performs iterations to solve the pressure equation until the error is small enough or the number of iterations is greater than the maximum number of iterations.
PROJ : Projects a given vector on a given plane.
SETFLD : Initialises variables at start of computation.
SETPAR : Reads input files.
SLAG : Computes one SOR-sweep to solve the pressure Poisson equation.
SOLVEP : Solves pressure from the pressure Poisson equation.
STREAM : Post-processing: Produces streamlines.
SURDEF : Initialises the volume of fluid function FS.
SURLAB : Labels the cells and velocities based on the free surface configuration.
TILDE : Computes the temporary vector field $\tilde{\mathbf{u}}$.
TRAFOS : Determine translation and rotation with respect to inertial system.
TUMBLE : Calculates the ship motion given the forces and moments exerted by the tank water.

VELBC : Computes the free surface velocities.
VFCONV : Computes the volume of fluid function FS at the new time level.
VTK : Post-processing: produces data for the use of VTK.

B.3 Common block variables

The variables that are used global are grouped in common blocks. Most of them are presented here in alphabetical order.

- **/ANTIROLL/**

Parameters concerning the motion of the anti roll tank.

XAMP(N), **XFRQ(N)**, **XPHS(N)** Amplitude, frequency and phase of the input signal of the tank motion.
XDCY(N) Start up parameter of tank motion.
XMOT(N), **XVEL(N)**, **XACC(N)** Motion, velocity and acceleration of the tank in six degrees of freedom N.
FORCED If **FORCED** is true, tank motion has a regular input.
MEASRD If **MEASRD** is true, tank motion has time series as input.

- **/APERT/**

AX(I, J, K) Edge-aperture A^x between cells (i, j, k) and $(i + 1, j, k)$.
AY(I, J, K) Edge-aperture A^y between cells (i, j, k) and $(i, j + 1, k)$.
AZ(I, J, K) Edge-aperture A^z between cells (i, j, k) and $(i, j, k + 1)$.
FB(I, J, K) Volume-aperture F^b in cell (i, j, k) .
FS(I, J, K), **FSN(I, J, K)** Volume of fluid function F^s in cell (i, j, k) at old and new time level.

- **/COEFP/**

DIV(I, J, K) Right-hand side of pressure Poisson equation in cell (i, j, k) .
CC(I, J, K) Coefficient of $p_{i,j,k}$ in pressure Poisson equation.
CXL(I, J, K), **CXR(I, J, K)** Coefficients of $p_{i-1,j,k}$ and $p_{i+1,j,k}$.
CYL(I, J, K), **CYR(I, J, K)** Coefficients of $p_{i,j-1,k}$ and $p_{i,j+1,k}$.
CZL(I, J, K), **CZR(I, J, K)** Coefficients of $p_{i,j,k-1}$ and $p_{i,j,k+1}$.

- **/COMMOI/**

LQMASS Mass of liquid.
LQCOMX, **LQCOMY**, **LQCOMZ** Center of mass of liquid, x -, y - and z -co-ordinate.
LQMOIXX, **LQMOIYY**, **LQMOIZZ**, Liquid's moments of inertia.
LQMOIXY, **LQMOIXZ**, **LQMOIYZ**

- **/COSYS/**

F1(R), **F2(R)**, **F3(R)** Unit vectors of the rotated co-ordinate system.
OMETN(R) Rotational velocity of the tank on the old time level.
GINRT, **FINRT** Equal 1 if the forces are in the earth-fixed co-ordinate system.
SHISYS Translation vector of the co-ordinate system.

- **/FILLAR/**, **/FLUXAR/** and **/FRCAR/**

The variables in these common blocks are used to create output for the post-processing.

- **/FLUID/**
 - RHO Density of fluid.
 - NU Dynamical viscosity coefficient
 - SIGMA Surface tension.
 - THETA Contact angle.
 - PATM Atmospheric pressure divided by the density RHO.

- **/FLXLAB/**
 - Variables for the computation of fluxes.

- **/FORCE/**
 - AMPLX, AMPLY, AMPLZ, Amplitude and frequency of tank motion
 - FREQX, FREY, FREZ (same as XAMP and XFRQ).
 - GRAVX, GRAVY, GRAVZ Gravitation vector, as read in the input file.
 - GRAV(R) Gravitation vector that changes in time.
 - OMET(R) Rotational velocity of the tank.
 - X0, Y0, Z0 Point of rotation.

- **/GRDSTR/**
 - XCONC, YCONC, ZCONC Center point of stretching.
 - XSTR, YSTR, ZSTR Stretch factors.

- **/GRIDAR/**
 - IMAX, JMAX, KMAX Number of grid points in x -, y - and z -direction.
 - X(I), Y(J), Z(K) Co-ordinates of grid points, such that the centre of a computational cell has co-ordinates $\frac{x(i)+x(i+1)}{2}$, $\frac{y(j)+y(j+1)}{2}$, $\frac{z(k)+z(k+1)}{2}$.
 - DXP(I), DYP(J), DZP(K) Mesh size: $DXP(I)=X(I)-X(I-1)$, etc.
 - DXU(I), DYV(J), DZW(K) Mesh size: $DXU(I)=0.5*(DXP(I)+DXP(I+1))$, etc.

- **/INTACT/**
 - RETAR22, RETAR24, Retardation functions used in the ship model.
 - RETAR42, RETAR44
 - T_RET(N) Vector containing the time series on which the retardation functions are known.
 - VELTANK Vector that contains the velocity of the tank during the past 15 seconds.
 - T_VEL Time series that belongs to VELTANK.
 - NRVELTANK Variable needed to store the tank velocity in VELTANK on the right point in time.
 - NMAX Length of the retardation functions and VELTANK.

- **/CONTRL/**

CONTROL	Integer with value 1 if control is on in input file.
LIQPS, LIQSB	Volume of liquid in port side and starboard tank.
HOLDWH	Equals 1 if the control valves are closed.
LIQPSOLD, LIQSBOLD	Volume of liquid in wing tanks at previous time.
DIFOLD	Old difference between successive volumes of liquid in a wing tank.
TFIXED, TFREE	Point in time when the valves are closed and opened respectively.
OMEMAX	Maximal roll velocity in last wave.
NATFREQ	Natural frequency of the tank.
ROLLFREQ	Roll frequency of the tank.
ZEROROLL	Equals 1 if the roll angle goes through zero.
TROLLO, TROLLMAX	Points in time when the roll angle is zero and maximal respectively.
AIRPSOLD, AIRSBOLD	Volume of air in wing tanks at previous time.
JPS, JSB	Indices of begin and end of the wing tanks.
FIRST	Equals 1 at the moment the valves are closed.
DIFVEL, DIFROLL	Difference between two successive roll velocities and roll angles respectively.
FRAC	Fraction of the maximal roll velocity (OMEMAX). If this fraction of OMEMAX is reached, the valves of the control system are opened.

- **/LABELS/**

ULABEL(I, J, K), ULABFS(I, J, K)	Geometry label and free-surface label of velocity u between cells (i, j, k) and $(i + 1, j, k)$
VLABEL(I, J, K), VLABFS(I, J, K)	Geometry label and free-surface label of velocity u between cells (i, j, k) and $(i, j + 1, k)$
WLABEL(I, J, K), WLABFS(I, J, K)	Geometry label and free-surface label of velocity u between cells (i, j, k) and $(i, j, k + 1)$
PLABEL(I, J, K)	Geometry label of pressure p in cell (i, j, k) .
PLABFS(I, J, K), PLABFSN(I, J, K)	Free-surface label of pressure p in cell (i, j, k) at old and new time level.

- **/LDSV/**

Variables which are used to make or read a restart file.

- **/LIQPAR/**

LIQCNF	Parameter that indicates whether you read the free surface from an input file or not.
LQXMIN, LQXMAX, LQYMIN, LQYMAX, LQZMIN	Input parameters which indicates the region where the water is located.
LQZMXL, LQZMXR	Indicates water height in port side and starboard wing tank respectively.

- **/MEASURE/**

Parameters needed to read the time series of the ship motion from input files if the variable MEASRD equals TRUE.

- **/NUMER/**
 - ALPHA Upwind parameter (0 central, 1 upwind).
 - EPS Required accuracy of pressure equation.
 - OMEGA Actual relaxation factor of SOR.
 - OMSTRT Starting value of the relaxation factor of SOR.
 - ITMAX Maximum number of iterations for an iteration process.
 - ITER The actual value of the number of iterations.
 - NOM
 - NORMP Norm of the pressure.
 - ITTOT Total amount of iterations during the simulation.
 - DIVL
- **/PHYS/**
 - U, UN The velocity in x -direction at old and new time level.
 - V, VN The velocity in y -direction at old and new time level.
 - W, WN The velocity in z -direction at old and new time level.
 - P The pressure.
- **/SHIPMO/**
 - ROLLFRQ, SWAYFRQ Excitation frequency of roll and sway motion.
 - A22, A33, A44, A24, A42 Added mass coefficients.
 - B22, B33, B44, B24, B42 Damping coefficients.
 - C22, C33, C44, C24, C42 Restoring coefficients.
 - AF2, AF3, AM4 Excitation forces and moment.
- **/SPACE/**
 - DOMAIN Type of flow domain (cube, cylinder, sphere etc.).
 - XMIN, XMAX Minimum and maximum x -co-ordinate of the mesh.
 - YMIN, YMAX Minimum and maximum y -co-ordinate of the mesh.
 - ZMIN, ZMAX Minimum and maximum z -co-ordinate of the mesh.
 - RADIUSY, RADIUSZ Radii for the round corners in the domain, to simulate a U-tank.
 - OBJECT Type of object in the flow.
 - OBXMIN, OBXMAX Minimum and maximum x -co-ordinate of the object.
 - OBYMIN, OBYMAX Minimum and maximum y -co-ordinate of the object.
 - OBZMIN, OBZMAX Minimum and maximum z -co-ordinate of the object.
 - SLOSH Is set to one in the input file if there is a free surface.
 - OBRY, OBRZ Radii for the round corners in the object, to simulate a U-tank.
- **/TANK/**
 - TKMASS Mass of the tank.
 - TKCOMX, TKCOMY, TKCOMZ Center of mass of the tank.
 - TKMOIXX, TKMOIYY, TKMOIZZ Moments of inertia of the tank.
 - TUMBLQ Is set to 1 in the input file, if you want to simulate with interaction.
 - DQDT, QT, INTQ Linear acceleration, velocity and motion of the tank in three co-ordinate directions.
 - DOMEDT, INTOME Rotating acceleration and motion of the tank, around the x , y and z -axis.
 - DTTANK, NRTANK Variables used for output reasons.

- **/TIME/**
 - TMAX Maximum simulation time.
 - T Current time.
 - DT Time step.
 - DTMAX Maximum time step according to diffusive time step limit.
 - CYCLE Current time cycle.
 - CFL The *CFL*-number.
 - CFLCNT Number of times that *CFL* is less than *CFLMAX*.
 - CFLQ If value is 1 then *DT* will be adjusted according to the *CFL*-condition.
 - CFLMIN Minimal *CFL*. If *CFL* ten successive time steps smaller, then time step is doubled.
 - CFLMAX Maximal *CFL*. If *CFL* is larger, then time step is halved.
 - TANKSTEPS Number of time steps to solve the tank's motion equations in one ComFlo time step.

B.4 Input files

The computer program ComFlo, adapted for the simulations of water flow in a U-tank, needs several input files, that are listed below.

Initialisation of variables The input file `comflo.in` contains initial values of many parameters in ComFlo. For example the tank and ship parameters, time step and maximum time, etcetera. The file has the following structure:

```

-----
dim*   cray   slosh   tumble   nttank   forcin   measin
3      0      1      1      1000    0        0
-----
domain  xmin   xmax   ymin   ymax   zmin   zmax   slip*  radiusy  radiusz
8      -0.5   0.5   -5.000  5.000  -3.100  1.300  0      1.20    1.50
-----
object  xmin   xmax   ymin   ymax   zmin   zmax   slip*  obry    obrz
4      -0.5   0.5   -2.600  2.600  -2.800  1.300  0      0.70   0.45
-----
liqcnf  lqxmin  lqxmax  lqymin  lqymax  lqzmin  lqzmxl  lqzmxr
1      -0.5   0.5   -5.000  5.000  -3.100  -3.100  -3.100
-----
rho     nu     sigma   theta
1000.0  1.0E-6  0.0    0.0
-----
tkmass  tkcomx  tkcomy  tkcomz  tkmoixx  tkmoiy  tkmoizz
1.0225E6 0.0    0.0    0.0    17525.7E3 196143.8E3 189126.7E3
-----
imax    jmax    kmax    xc      yc      zc      sx      sy      sz
1      40     20     0.0    0.0    0.0    1.0    1.0    1.0
-----
eps     omega   itmax   alpha   orde4*  feab1   feab2   nrintp  exact*

```

```

1.0E-5  1.0    10000  1.0    0      1.0    0.0    1      0
-----
dt      tmax    cfl     cflmin  cflmax  divl    tanksteps
0.01   100    0       0.05   0.25   0       1
-----
control natfreq
0      0.56
-----
gravx   gravity gravz   ginrt   finrt
0.0    0.0    -9.81  1       1
-----
amplx   freqx   amply   freqy   amplz   freqz   u0*    v0*    w0*
0.0    0.0    0.0    0.0    0.0    0.0    0.0    0.0    0.0
-----
q0x     q0y     q0z
0.0    0.0    0.0
-----
omex    omev    omez    tup*    tdown*  x0      y0      z0
0.0    0.0    0.0    0.0    0.0    0.0    0.0    0.0
-----
load    nsave
0      10
-----
npavs   tbavs*  comavs  npmatl  tbmatl* npvtk   nprnt   ntcom   ntmoi
0      0.0    0       50     0.0    0       100    300    300
-----
avs pathname:
data/
matlab pathname:
data/
vtk pathname:
data/
-----
nfillb  ntfill
1      400
xl      xr      yl      yr      zl      zr
-0.5   0.5    2.6    5.0    -3.1   1.3
-----
nfrcb   ntfrc
1      400
xl      xr      yl      yr      zl      zr
-0.5   0.5    -5.0   5.0    -3.1   1.3
-----
nfluxb  ntflux
1      400
xl      xr      yl      yr      zl      zr
-0.5   0.5    0.0    0.0    -3.1   -2.8

```

```

-----
npartp  npartl  npartc  ntpart
0        0        0        0
xpt     ypt     zpt     tstrt           <- points
xl      xr      yl      yr      zl      zr      tstrt         <- lines
xc      yc      zc      radius  orient  tstrt           <- circles
-----

nmntrp  nmntrl  nmntrc  ntmntr
0        0        0        0
xpt     ypt     zpt           <- points
xl      xr      yl      yr      zl      zr           <- lines
xc      yc      zc      radius  orient           <- circles
-----

```

Input files that prescribe the motion of the tank There are two ways to prescribe the motion of the tank. First you can describe the motion of the tank by a sinus function, that is used by ComFlo to compute every time step the velocity and acceleration of the tank. In this case ComFlo needs the input file `antiro11.inp` which contains the amplitude, frequency, phase and a start-up parameter to define the tank motion and the maximal time. This file is needed when the parameter `forcin` in the input file `comflo.in` equals 1.

The other way is to give the motion of the tank as a time series. In this case the parameter `measin` in `comflo.in` equals 1. Then ComFlo determines the motion of the tank by interpolating using the time series. These time series are given in input files `sway.ms.dat`, `heave.ms.dat` and `roll.ms.dat` that contain sway, heave and roll velocities and accelerations respectively.

Files used for the interaction To solve the equations of the linear ship motion model ComFlo needs two input files: `shipmo.in` and `retar.dat`. The file `shipmo.in` contains values of the coefficients in the equations and looks like this:

```

-----
rollfrq  swayfrq  A22      A33      A44      A24      A42
0.4      0.3      282741.0 0.0      0.233075E+07 -95362.1 14832.8
-----

B22      B33      B44      B24      B42
0.0      0.0      1800.0E3 0.0      0.0
-----

C22      C33      C44      C24      C42      F2      F3      AM4
0.0      0.0      8526.3E3 0.0      0.0      0.0      0.0      93.0E3
-----

```

The file `retar.dat` contains the retardation functions to compute F_y^{rad} and M_x^{rad} . Both files are only needed if the parameter `tumble` in the input file `comflo.in` equals 1.

B.5 Output files and post-processing

ComFlo produces a lot of data for post-processing reasons. Most of them are put into files that are used by Matlab to visualise the results. For this reason a graphical user interface is

built in Matlab. The main control menu is shown in figure B.1. Below the output files are listed. When we say it can be visualised by Matlab, it can be done using the graphical interface; of course, by explicitly programming elementary Matlab commands more visualisation options are possible.

- **auto.sav.gz** In this file the variables needed for a restart are put.
- **com.dat** This file contains a time history of the center of mass of the liquid. We can visualise this, using Matlab.
- **control.dat** The time point when the valves of the control system are closed and opened is written **control.dat**
- **dthist.dat** In this file the changes of the time step during the simulation is stored with the time and time cycle when it changes. Using this file, Matlab can visualise the time versus cycle, the time step versus time and the time step versus cycle.
- **fill**.dat** In this file time histories of the total volume, the liquid volume and the percentage of liquid in fillbox ** are stored. Matlab is able to visualise these quantities and can derive the liquid height in fillbox ** in three directions.
- **flux**.dat** This file contains a time history of the flux through a plane, defined by a box ** in the input file **comflo.in**. Pictures can be made, using Matlab.
- **frc**.dat** This file contains time histories of the forces in the three coordinate directions and moments around the three axes. This can be visualised by Matlab.
- **iter.dat** This file contains time histories of the cycle number, the number of iteration per cycle and the total number of iterations. These histories can be visualised using Matlab.
- **kinetic.dat** This file contains the time, the cycle number and the kinetical energy in that cycle. This can be visualised by Matlab.
- **moi.dat** In this file the moments of inertia of the fluid are stored. These quantities can be visualised using Matlab.
- **motion.dat** This file contains time histories of the motion of the tank, namely the sway, heave and roll motion.
- **tank.dat** This file contains motions, velocities and accelerations of the tank in all six degrees of freedom. ComFlo only produces the file when we simulate with interaction between fluid and tank motion. So when the parameter **tumble** in the input file equals 1. The quantities in this file can be visualised using Matlab.

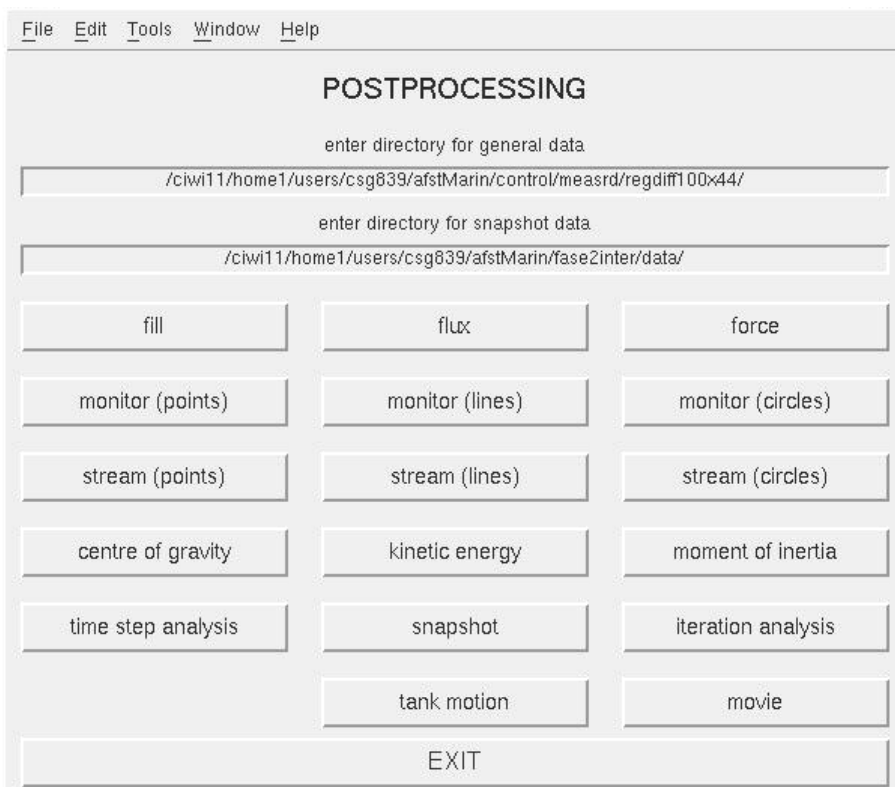


Figure B.1: *Main menu of graphical user interface in Matlab*

Bibliography

- [1] Anonymous. Stabiliser and Anti-heeling Tank System Combined. *Naval Architect*, (3), 1979.
- [2] E.F.G.van Daalen, K.M.T. Kleefsman, J. Gerrits, H.R. Luth, and A.E.P. Veldman. Anti-Roll Tank Simulations with a Volume of Fluid (VOF) Based Navier-Stokes Solver. *Symposium on Naval Hydrodynamics, Val de Rueil*, September 2000.
- [3] E.F.G.van Daalen, A.G. van Doeveren, P.C.M. Driessen, and C.Visser. Two-dimensional free surface anti-roll tank simulations with a Volume Of Fluid based Navier-Stokes solver. Report No. 15306-1-OE, Maritime Research Institute Netherlands, October 1999.
- [4] E.F.G.van Daalen and J.H. Westhuis. 3D fluid sloshing in rectangular containers - Validation of a Volume Of Fluid based Navier-Stokes solver. Report No. 16131-2-RD, Maritime Research Institute Netherlands, May 2000.
- [5] S.B. Field and J.P. Martin. Comparative Effects of U-Tube and Free Surface Type Passive Roll Stabilisation Systems. *Naval Architect*, (2), 1976.
- [6] J. Gerrits. Fluid Flow in 3-D Complex Geometries - A Cartesian Grid Approach. Master's thesis, Rijksuniversiteit Groningen, 1996.
- [7] J. Gerrits. Three Dimensional Liquid Sloshing in Complex Geometries. Master's thesis, Rijksuniversiteit Groningen, 1996.
- [8] J. Gerrits and A.E.P. Veldman. Numerical Simulation of Coupled Liquid-Solid Dynamics. In *Proceedings Eccomas 2000*, Barcelona, 11-14 September 2000.
- [9] C.W. Hirt and B.D. Nichols. Volume of Fluid (VOF) Method for the Dynamics of Free Boundaries. *J. Comput. Phys.*, 39, 1981.
- [10] R.B. Pember, J.B. Bell, P. Colella, W.Y. Crutchfield, and M.L. Welcome. An Adaptive Cartesian Grid Method for Unsteady Compressible Flow in Irregular Regions. *J. Comput. Phys.*, 120, 1995.
- [11] C. Stigter. The Performance of U-tanks as a Passive Anti-rolling Device. Report Nr. 81 S, Nederlands scheeps-studiecentrum TNO, 1966.
- [12] A.E.P. Veldman. Numerieke stromingsleer. Lecture notes, Rijksuniversiteit Groningen, 1994.
- [13] S. Yamaguchi and A. Shinkai. An Advanced Adaptive Control System for Activated Anti-Rolling Tank. *International Journal of Offshore and Polar Engineering*, 5(1), 1995.

- [14] Z. Zhong, J.M. Falzarano, and R.M. Fithen. A Numerical Study of U-Tube Passive Anti-Rolling Tanks. *Proceedings of the International Offshore and Polar Engineering Conference*, 3, 1998.